Facies (2024) 70:5
https://doi.org/10.1007/s10347-023-00679-2

ORIGINAL ARTICLE

Biostratigraphy and paleoecology of the upper Badenian carbonate and siliciclastic nearshore facies in the Vienna Basin (Slovakia)

Michal Jamrich[1] · Samuel Rybár[1,2] · Andrej Ruman[1] · Marianna Kováčová[1] · Natália Hudáčková[1]

Received: 19 June 2023 / Accepted: 27 December 2023 / Published online: 29 January 2024

Abstract

This study provides a comprehensive examination of algal bioherm structures, including reefs and carpets that contain nannoplankton and foraminifera, originating from the upper Badenian (middle Miocene) strata of the Vienna Basin in the Central Paratethys. These lithofacies primarily consist of the carbonate red algal genus *Lithothamnion*. Through an integrated approach that combines calcareous nannoplankton, foraminifera, sedimentology, and palynology, the study explores the Serravallian (upper Badenian) sediments from the Vienna Basin. The biostratigraphic age, consistent with the NN6 and CPN9 zones, is further corroborated by $^{87}Sr/^{86}Sr$ dating. This research highlights the importance of taphonomic processes and paleoecological proxies in small-scale characterization and detecting short-term shifts within paleoenvironmental conditions. These unique bioherm structures enable a novel description of a limestone formation within the Vienna Basin (Sandberg Formation), which seems pervasive across the Central Paratethys region. The findings uphold the hypothesis of a profound connection between the Mediterranean and Central Paratethys via the Trans-Tethyan Trench Corridor, bolstered by upwelling conditions observed in the eastern perimeter of the Vienna Basin. Two main inhibitory mechanisms for carbonate growth in the Upper Badenian within the Central Paratethys area are confirmed: the first is a substantial siliciclastic influx from the Alps and Carpathians, supported by the ongoing rifting of the Vienna and Danube Basins; the second is the propagation of evaporites in the Transcarpathian and Transylvanian Basins leading to precipitation, which disrupts carbonate growth. This investigation underlines the intertwined relationship between regional geodynamics and carbonate sedimentation processes during the Miocene.

Keywords Central Paratethys · Serravallian · Lithofacies · Nannoplankton · Foraminifera

Introduction

During the Serravallian, significant paleoenvironmental changes occurred in the Central Paratethys (CP) Sea, as evidenced by studies from Kováč (2000), Piller et al. (2007, 2022), Hohenegger et al. (2014), Ruman et al. (2017), Nováková et al. (2020), and Kranner et al. (2021a, b). The northeast corner of the Vienna Basin (VB) has been extensively studied through local paleontological research at sandpits and road cuts, as documented by Mišík (1974), Švagrovský (1981), Baráth et al. (1994), Sabol and Holec (2002), Hyžný et al. (2012), Bitner et al. (2014), Pivko et al. (2017), Ruman et al. (2017), and Šujan (2019). However, a comprehensive study synthesizing these findings is lacking. The red algal genus *Lithothamnion* significantly influenced the local lithofacies, forming reefs, carpets, and bioherms of upper Badenian (Schaleková 1969, 1973). These limestones are younger than the well-studied Leitha Formation limestones (Kysela 1988; Schmid et al. 2001; Mišík and Reháková 2009; Wiedl et al. 2013, 2014; Harzhauser et al. 2020). The discussed limestones, sometimes referred to as the St. Margarethen (Harzhauser et al. 2020); and Rákos limestones (Császár 1997), correlate with the NN6 lower part and *Bulimina–Bolivina* Zone (younger than 13.53 Ma), as indicated by Hudáčková et al. (2003), Jamrich and Halásová (2010). This study aims to reassess archival and new

✉ Michal Jamrich
michal.jamrich@uniba.sk

[1] Department of Geology and Paleontology, Faculty of Natural Sciences, Comenius University Bratislava, Mlynská Dolina, Ilkovičova 6, 842 15 Bratislava, Slovakia

[2] Department of Geodesy and Mine Surveying, Faculty of Mining and Geology, Technical University of Ostrava, 17. Listopadu 2172/15, Poruba, 708 00 Ostrava, Czech Republic

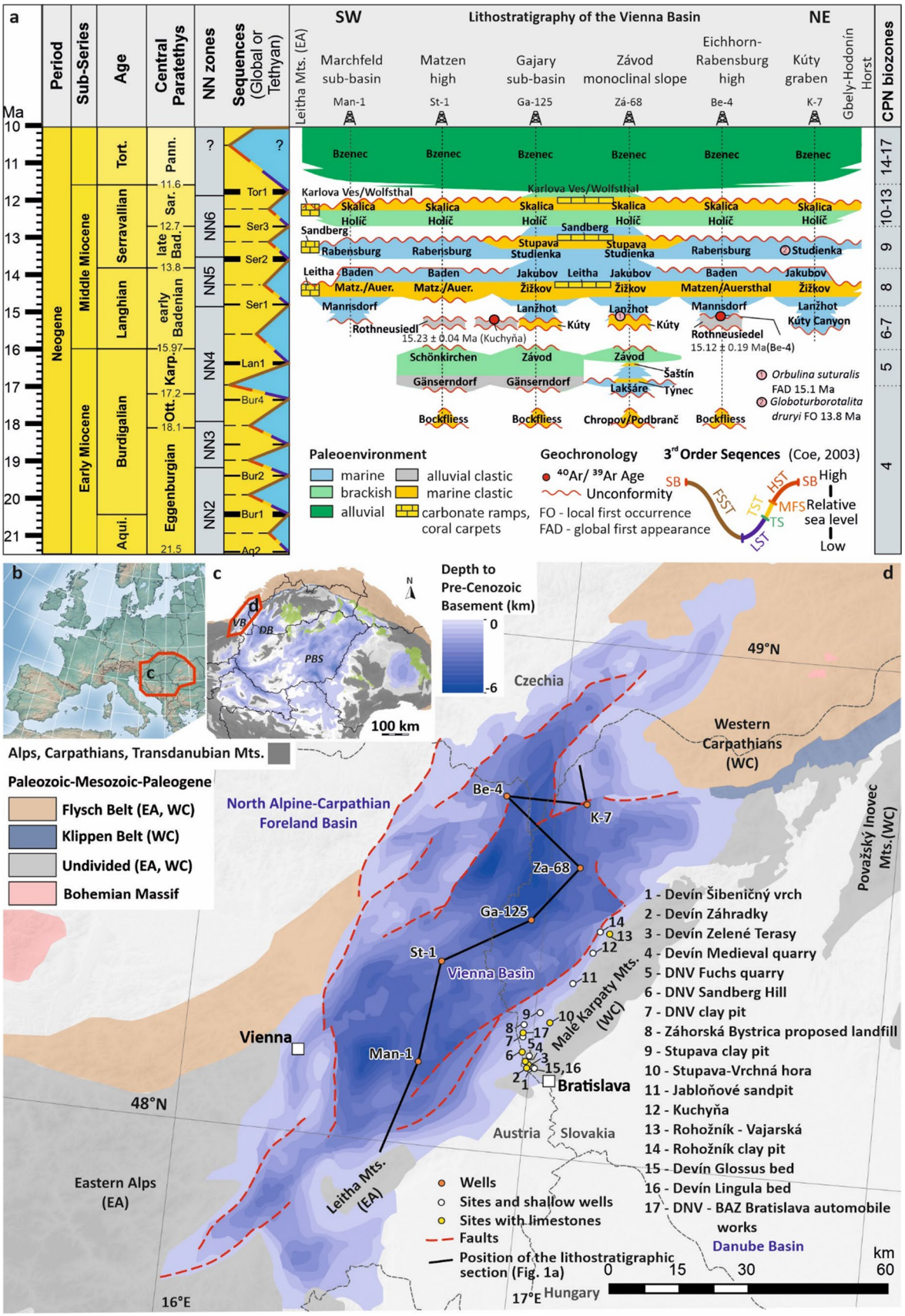
a
Period
Sub-Series
Age
Central Paratethys
NN zones
Sequences (Global or Tethyan)
Ma
Neogene
Middle Miocene
Early Miocene
Tort.
Serravallian
Langhian
Burdigalian
Aqui.
Pann.
late Bad.
early Badenian
Karp.
Ott.
Eggenburgian
Sar.
11.6
12.7
13.8
15.97
17.2
18.1
21.5
NN6
NN5
NN4
NN3
NN2
Tor1
Ser3
Ser2
Ser1
Lan1
Bur4
Bur2
Bur1
Aq2
SW
Lithostratigraphy of the Vienna Basin
NE
Leitha Mts. (EA)
Marchfeld sub-basin
Matzen high
Gajary sub-basin
Závod monoclinal slope
Eichhorn-Rabensburg high
Kúty graben
Gbely-Hodonín Horst
Man-1
St-1
Ga-125
Zá-68
Be-4
K-7
CPN biozones
14-17
10-13
9
8
6-7
5
4
Bzenec
Karlova Ves/Wolfsthal
Skalica
Holíč
Sandberg
Rabensburg
Stupava
Studienka
Leitha
Baden
Matz./Auer.
Jakubov
Žižkov
Matzen/Auersthal
Manrsdorf
Lanžhot
Kúty
Kúty Canyon
Rothneusiedl
15.23 ± 0.04 Ma (Kuchyňa)
15.12 ± 0.19 Ma(Be-4)
Schönkirchen
Závod
Gänserndorf
Šaštín
Týnec
Lakšáre
Bockfliess
Chropov/Podbranč
1 Orbulina suturalis FAD 15.1 Ma
2 Globoturborotalita druryi FO 13.8 Ma
Paleoenvironment
marine
brackish
alluvial
alluvial clastic
marine clastic
carbonate ramps, coral carpets
Geochronology
40Ar/ 39Ar Age
Unconformity
FO - local first occurrence
FAD - global first appearance
3rd Order Seqences (Coe, 2003)
SB
FSST
LST
TST
HST
MFS
TS
High
Relative sea level
Low
b
c
d
VB
DB
PBS
100 km
N
Depth to Pre-Cenozoic Basement (km)
0
-6
49°N
48°N
16°E
17°E
Czechia
Western Carpathians (WC)
Považský Inovec Mts.(WC)
Alps, Carpathians, Transdanubian Mts.
Paleozoic-Mesozoic-Paleogene
Flysch Belt (EA, WC)
Klippen Belt (WC)
Undivided (EA, WC)
Bohemian Massif
North Alpine-Carpathian Foreland Basin
Vienna Basin
Vienna
Bratislava
Austria
Slovakia
Hungary
Malé Karpaty Mts. (WC)
Eastern Alps (EA)
Leitha Mts. (EA)
Danube Basin
1 - Devín Šibeničný vrch
2 - Devín Záhradky
3 - Devín Zelené Terasy
4 - Devín Medieval quarry
5 - DNV Fuchs quarry
6 - DNV Sandberg Hill
7 - DNV clay pit
8 - Záhorská Bystrica proposed landfill
9 - Stupava clay pit
10 - Stupava-Vrchná hora
11 - Jabloňové sandpit
12 - Kuchyňa
13 - Rohožník - Vajarská
14 - Rohožník clay pit
15 - Devín Glossus bed
16 - Devín Lingula bed
17 - DNV - BAZ Bratislava automobile works
Wells
Sites and shallow wells
Sites with limestones
Faults
Position of the lithostratigraphic section (Fig. 1a)
km
0
15
30
60

◂**Fig. 1** **a** Miocene Chrono/lithostratigraphic framework of the Vienna Basin and the location map of the studied sections. Timescale adapted from Krijgsman and Piller (2012); the lithostratigraphic details follow Špička (1966), Baráth et al. (1994), Vass (2002), Kováč et al. (2004, 2007, 2008a, b), Fordinál et al. (2013), Harzhauser et al. (2019, 2020, 2022), Csibri et al. (2022); global sequences after Haq et al. (1988) and Hardenbol et al. (1998), Coe (2003); CPN Zonation from Cicha et al. (1975); FAD—*O. suturalis* from Wade et al. (2011), FO *G. druryi* after Hudáčková et al. (2013), Šarinová et al. (2021). **b** Location of the Pannonian Basin System within Europe. **c**, **d** Position of the Vienna Basin within the Alpine–Carpathian–Pannonian region

upper Badenian sections to understand the eco-space genesis and the variability between clastic and carbonate facies in the Slovak part of VB. It also examines shallow water formations, using their genesis as a key distinguishing factor. In addition, the study seeks to map these limestone occurrences throughout the CP and elucidate the mechanisms of their origin.

Geology

The deposits below the studied interval consist of the Jakubov/Baden formations, extending from the inner to outer shelf, and from the carbonate Leitha Formation. These formations, older than 13.8 Ma (Vass 2002; Fordinál et al. 2013; Harzhauser et al. 2020), are situated below the Langhian/Serravallian boundary in the Central Paratethys (CP). The 13.8 Ma numeric boundary date is supported, e.g., by Lukács et al. (2015) in Hungary and Šarinová et al. (2021) in Slovakia. This study primarily focuses on the late Badenian strata, characterized by the muddy Studienka/Rabensburg formations, dated younger than 13.8 Ma. These formations comprise a variety of environments from the outer shelf to inner shelf and lagoons, as noted by Špička (1966), Vass (2002), Kováč et al. (2008a), Harzhauser et al. (2020), and Piller et al. (2022). The Sandberg Member of the Studienka Formation, representing marginal inner shelf facies, consists of conglomerates and sandstones intercalated with algal limestone beds (Baráth et al. 1994). Notable limestone types include algal-biodetritic limestone, as found in the Kúty-45 well (Kováč et al. 2008b). This environment, initially sandy coastal plains, evolved with rising sea levels, promoting the growth of *Lithothamnion* reefs. The age of these deposits is determined through analyses of mollusk, foraminifera, nannofossil assemblages, and $^{87}Sr/^{86}Sr$ dating (Hudáčková et al. 2003; Hyžný et al. 2012; Fordinál et al. 2014; Harzhauser et al. 2020; Harzhauser 2022a, b, c). The overlying Sarmatian-age Holíč Formation, encompassing muddy and sandy layers, changes from outer shelf to deltaic settings (Vass 2002; Kováč et al. 2008a; Hudáčková et al. 2021). The basin margin features the Karlova Ves Member in Slovakia and its Austrian equivalent, the Wolfsthal Member, comprise sandy-coquina and oolitic limestones, transitioning into upper cross-bedded sands (Nagy et al. 1993; Vass 2002; Harzhauser and Piller 2004; Harzhauser 2022a, b, c). Thus, the environment, interpreted as bryozoa-serpulid reefs (Harzhauser and Piller 2004; Piller and Harzhauser 2023) was later submerged by fluvial ecosystems.

Methods

The shallow-water sedimentary structures and paleoenvironment were identified based on Rossi et al. (2017) and Pellegrini et al. (2020). Field facies analysis followed standard procedures (Boggs 2006; Nichols 2009). Thin sections were prepared from samples ranging from algal limestones to sandstones and examined under a polarizing microscope. They were utilized for sedimentary microstructure description and foraminifera identification.

Samples were picked from various sedimentary environments (Figs. 1, 2). From Zelené terasy (**ZT**) construction site 17 samples, Devínska Nová Ves–Bratislava automobile works–BAZ (**BAZ**) 2, Stupava–Vrchná hora (**VH**) 5, Jabloňové (**J**) 11, Kuchyňa (**K**) 1 and Rohožník–Vajarská (**RV**) 2 samples were collected for biostratigraphy and paleoecology analyses. All essential layers were measured, labeled, and photo documented.

Calcareous nannofossils were studied in samples from **ZT**5, 8–12, 15, 17; **BAZ**1; **VH**1, 5; **J**4, 7–9; **K**1; and **R**1, 2. Preparation and analysis follow the method of Bown and Young in Bown (1998). Further adjustments were made using methods described in Nováková et al. (2020). Counts were transposed in percentages to show the composition of the assemblages. Systematic identification and taxonomy follow Young (1998) and Young et al. (2017). Standard NN zones are after Martini (1971) and Hilgen et al. (2012). Paleoenvironmental characteristics follow the concept of Ćorić and Hohenegger (2008) and Auer et al. (2014).

Foraminiferas were examined from **ZT**1–17; **BAZ**1–2; **VH**1–5; **J**1–10; **K**1. Samples were prepared sensu Ruman et al. (2017). Taphonomic analysis was applied using the methods of Holcová (1999). Foraminiferas were measured using a micrograph scale. Systematic identification and taxonomy follow Cicha et al. (1998) and Hayward et al. (2023).

Palynological analysis was performed on samples from **ZT**4–12 and 14–17. Processing utilized standard methods described in Doláková et al. (2021). Microscopy and imaging were performed using a Zeiss Axioskop 40 (400–630 × magnification), Axiocam ERc 5 s camera, and SEM microscope QUANTA FEG250.

Newly obtained data (foraminifera and calcareous nannoplankton) to evaluate the eco-space variability were combined with datasets from published results from Rohožník

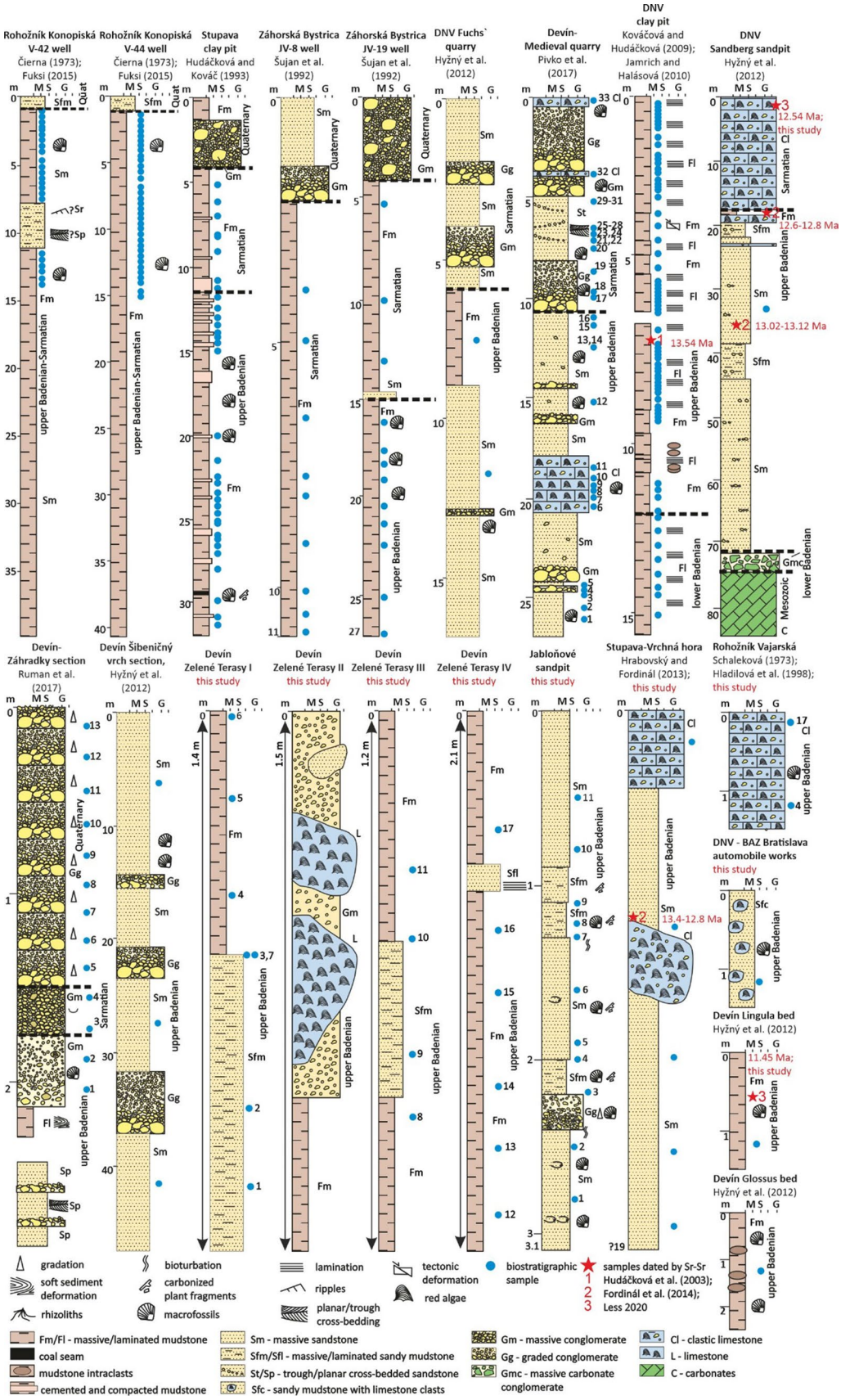

Fig. 2 Lithological columns of the discussed sections (studied and archived). Note, for previously published results, see references within the figure

Konopiská (**RK**) shallow wells V-42, V-44 (Čierna 1973; Fuksi 2015), Záhorská Bystrica landfill (**ZB**), and Stupava clay pit (**SC**) shallow wells (Šujan et al. 1992; Hudáčková and Kováč 1993), Devínska Nová Ves clay pit (**D**) (Kováčová and Hudáčková 2009; Jamrich and Halásová 2010), Devínska Kobyla Hill localities (**DK, L, FL, G, DSi, S**) (Hyžný et al. 2012), Stupava–Vrchná hora (**VH**) (Hrabovský 2013; Hrabovský and Fordinál 2013), Devínska Kobyla Medieval quarry (**MQ**) (Pivko et al. 2017), and Devín–Záhrady construction site (**DZ**) (Ruman et al. 2017) (Fig. 2).

The statistical coupling analysis was applied based on the established taxonomical concept for calcareous nannoplankton (Jamrich and Halásová 2010). Due to the limitation of various approaches to foraminifera species determination in different publications (Čierna 1973; Kováčová and Hudáčková 2009), some species were grouped based on similar ecological preferences. Species of the *Bulimina* genus were grouped to *Bulimina* ex gr. *elongata*, species of the *Bolivina* genus were grouped according to their morphology into 1) flat smooth and 2) inflated cancellate groups, species of the genus *Elphidium* were split into 1) keeled and 2) non-keeled elphidia (sensu Haynes 1981; Murray 2006). Diversity indices (SSD- simple species number diversity), Shannon_H, Simpson, and Fisher α were used (Hammer et al. 2001).

Statistical methods, such as non-metric multidimensional scaling (NMDS), cluster analysis, and principal component analysis (PCA) (Bray Curtis similarity—BC) were applied on benthic foraminifera (with foraminiferal number ≥ 70) and calcareous nannoplankton, and processed by Paleontological Statistics, ver. 4. 03 (PAST) (Hammer et al. 2001) and POLPAL software (Walanus and Nalepka 1999) for distribution charts. Data were exported (Supplements 1, 2) from Microsoft Excel, Microsoft Access database adjusted by Hudáčková and Hudáček (2001).

$^{87}Sr/^{86}Sr$ dating

The value of the $^{87}Sr/^{86}Sr$ ratio from Eocene to present, characterized by a steep marine Sr isotope curve, can be calibrated to the numerical time scale with an accuracy of up to 500,000 years, although in the period between 15 and 13 Ma, the change in $^{87}Sr/^{86}Sr$ ratio slowed down significantly; thus, numerical dating is also much more imprecise. Freshwater input affects the normal marine $^{87}Sr/^{86}Sr$ ratio, which causes a problem. The period of normal saline waters in the CP lasted from the Oligocene to the end of the Badenian (~ 12.7 Ma), so the SIS for dating these formations could be applied (Less 2020). $^{87}Sr/^{86}Sr$ results of Fordinál et al. (2014) and Less (2020) are referenced within this paper.

Results

Sedimentary facies

ZT—description

The Zelené Terasy (**ZT**) composite profile is situated on the eastern end of Devín district (48°10′35.47″ N, 16°59′48.29″ E). The profile comprises four sections, designated I to IV (Figs. 2, 3). These sections were formerly a part of a construction pit. Section I, located at the southern end of the profile, starts with an ochre-colored, massive, fossiliferous sandy mudstone (**Sfm**; refere to Figs. 2 and 3 for facies codes). **Sfm** sharply and angularly contacts a massive, fossiliferous, bioturbated brown-gray mudstone (**Fm**; Fig. 3). **Fm** facies extends into section II, where it is in an erosive contact with a matrix-supported, poorly sorted, and poorly rounded conglomerate that contains clasts ranging in size from granules to boulders. This facies is around 130 cm thick and extends to the top of the section. The matrix is sandy, with abundant bioclasts. Limestone and sandstone are present both in detrital and clast form (**Gm**; Fig. 3). The algal-biodetritic limestones represent redeposits and can be described as white patches with ochre coating and sandy mudstone matrix. Clasts of these limestones can reach from few centimeters up to several meters in diameter (Fig. 3). Section III comprises a 40 cm thick gray massive mudstone (**Fm**; Fig. 3) overlain by a thin (1–2 cm) red layer containing iron oxides. A 40 cm thick, mauve-colored massive, fossiliferous sandy mudstone follows (**Sfm**; Fig. 3). Above, a brown-gray massive, fossiliferous mudstone (**Fm**) occurs again. Section IV is located at the northernmost end of the profile and begins with a 30 cm thick gray mudstone (**Fm**). In the middle part of the section, a 10 cm thick, indistinctly laminated sandy mudstone appears (Fig. 3; **Sfl**).

J—description

The Jabloňové section **(J)** is situated in an abandoned sandpit south of the Jabloňové village (48°20′26.67″ N, 17°6′6.49″ E). The section (Fig. 4) commences with a 70 cm thick massive, fossiliferous, bioturbated, medium- to fine-grained sand facies well-sorted and rounded, with few plant fragments (**Sm**; refer to Fig. 5 for facies codes). Above this facies is a 20 cm thick graded, fossiliferous, bioturbated, matrix-supported gravel with granule to pebble-sized well-sorted and rounded clasts (**Gg**). An

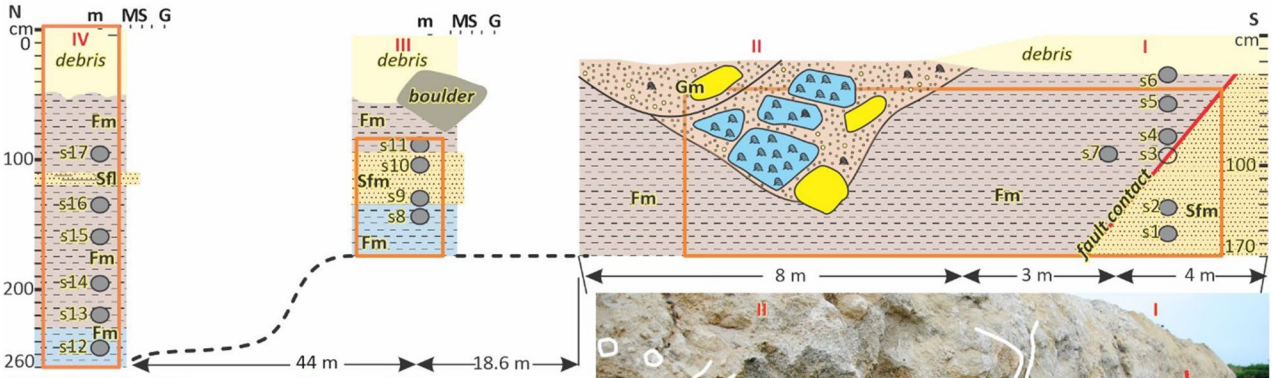

limestone block | sandstone block | massive conglometate | massive mudstone | massive/laminated sandy-mudstone | debris

b

Lithofacies code	Lithofacies	Sedimentary textures	Depositional process	Interpretation/paleobathymetry
Gm	Matrix supported, granule to boulder sized congl. with poorly sorted and rounded clasts	Massive or week grading	Terrestrial debris flow (scour fill)	Costal plain (0 - and above sea level m)
Sfl/Sfm	Fossiliferous sandy-mudstone	Occasional indistinct lamination	Wave and/or Tide action	Shoreface (0-6 m)
Fm	Fossiliferous bioturbated multi-colored mudstone	Massive	Suspension	Inner Shelf (6-60 m)

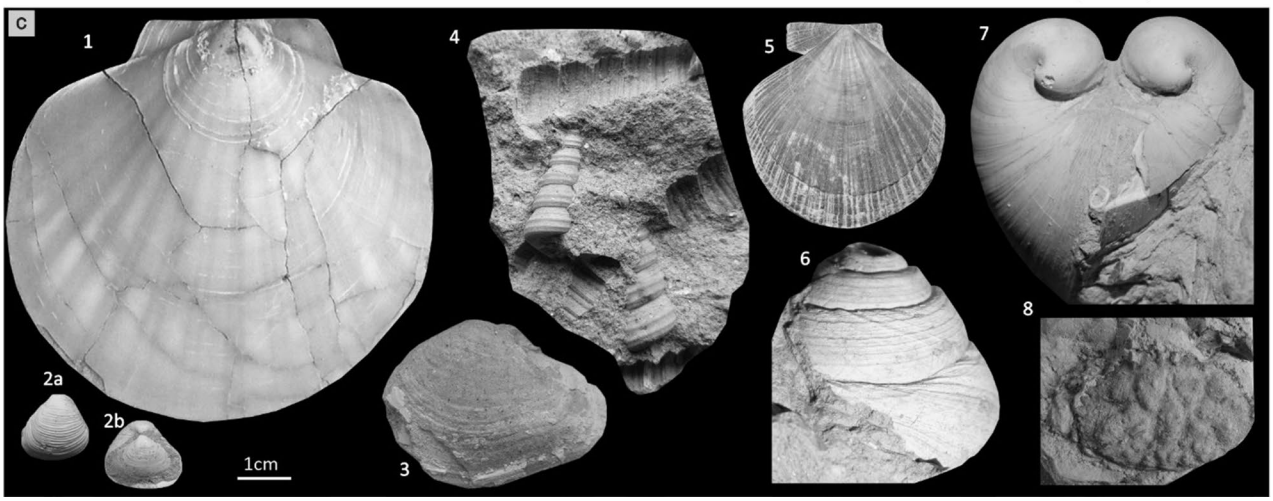

◂**Fig. 3** ZT studied profile. **a** Location map adopted from Google Earth Pro, Image © 2022, yellow circle and line show the location and orientation of the profile on the map; **b** section with facies description and details; the white lines represent the internal structure and boundaries of a scour fill and other lithofacies intervals. Paleobathymetries are implied from the interconnection of the study by Pellegrini et al. (2020) with Rossi et al. (2017), Boggs (2006), and Nichols (2009). Nevertheless, please note that the paleobathymetries are only orientational; **c** 1—*Parvamussium cristatellum*, 2a,b—*Varicorbula gibba*, 3—*Thracia convexa*, 4—*Turritella* sp., 5—*Karnekampia lilli*, 6—*Paroxystele orientalis*, 7—*Glossus humanus*, 8—*Tasadia carniolica*

alternation of **Sm** and **Sfm** facies characterizes the remaining 220 cm of the section. **Sfm** facies comprise massive, fossiliferous, bioturbated muddy sands with a few plant fragments.

BAZ—description

The BAZ section (Fig. 6) is north of the **Devínska Nová Ves–Bratislava automobile works (BAZ)** (48°14′36.75″ N, 16°58′22.09″ E). The facies comprise massive, bioturbated, fossiliferous sandy mudstones with bivalve rock cores and *Lithothamnion* clasts (**Sfm**). These facies extend deeper into the substratum, spanning more than 70 cm in thickness. The section then continues with a weathered layer (~ 30 cm thick), followed by a soil layer at the top (~ 30 cm thick).

Nannoplankton

Eight samples of the ZT section (Fig. 2) were studied (ZT5, 8–12, 15, 17). Thirty-four Neogene taxa were determined, abundance and preservation are moderate. The most abundant samples, 11, 5, 10, 8, were dominated by small and medium-sized reticulofenestrids (Fig. 7, Supplement 1) up to 68.45% in sample 10 (*Reticulofenestra haqii* 28.88–68.45%). Apart from autochthonous, rare reworked Lower Miocene, Paleogene, Cretaceous taxa were observed represented by *Helicosphaera ampliaperta*, *Reticulofenestra lockeri*, *Helicosphaera compacta*, *Micula staurophora*, *Prediscosphaera cretacea*, *Cribrosphaerella ehrenbergii*. Simpson diversity ranges from 0.3975 to 0.801, with the highest in sample 9. Stratigraphically important taxa include *Orthorhabdus rugosus* (ZT9–12, 17) and *Braarudosphaera bigelowii parvula*, *Helicosphaera wallichii*, *R. sicca*, *Sphenolithus abies.*

Cluster analysis of percentages by Ward's method (Fig. 8a) split ZT samples into three clusters (distance level 27, Supplement 3a), and similar three clusters were distinguished on distance level 60 within entire new data matrix (Fig. 8b, Supplement 3b). NMDS analysis (Fig. 9) based on Bray Curtis similarity and proved stress by Sheppard diagram 0.1054 grouped studied assemblages into three groups: group 1 – ZT samples with the prevalence of *R. haqii*, group 2 – J4, 7, 8 and K1 samples *C. pelagicus*, group 3 – BAZ1, J9, R1, R2 and VH5 samples with high equitability (Supplement 1).

NMDS percentages correlation of nearby localities (Fig. 10a) with Sheppard diagram stress 0.1244 shows three groups. Reticulofenestrids dominated Group 1 (mainly composed of D and ZT). Group 2 (S, J, K samples) with *C. pelagicus* and *R. pseudoumbilicus*, and Group 3 (BAZ1, R, VH5) with the prevalence of *R. minuta*. Samples J9 and VH1 (not shown) are considered outliers. PCA (Fig. 10b) of ZT and all sites used for correlation distinguish three main groups. G1 with mainly D, ZT10, S1.1 samples discriminated by *R. haqii*, G2 dominated by S, ZT, J, K with *C. pelagicus*, and G3 with D, ZT, J, BAZ1, VH, R with *R. minuta*.

New calcareous nannoplankton data were combined, analyzed, correlated, and evaluated with datasets from published results. The listing of additional results is in alphabetical order:

Devínska Nová Ves–Bratislava automobile works (BAZ)—new data (Figs. 2, 6). The exceptionally rich nanno sample consists mainly of *R. minuta* (46.51%) and *C. pelagicus* (27.2%). Stratigraphic important taxa are *Pontosphaera japonica*, *R. sicca*, *R. pseudoumbilicus*, *Calcidiscus premacintyrei*, *S. abies*, *Coronocyclus nitescens* (elliptical) (Supplement 1).

Jabloňové sandpit (J)—new data (Figs. 2, 4). Four samples (4, 7–9) were analyzed for nannofossils dominated by *C. pelagicus* (J7 59.15%) and stratigraphic important taxa, including *H. wallichii*, *Orthorhabdus serratus*, *O. rugosus*, *R. pseudoumbilicus*, *S. abies*, *Triquetrorhabdulus milowii* (Supplement 1).

Kuchyňa (K)—new data. One sample studied for nannofossils, and foraminifera includes mainly *C. pelagicus* (47.61%), *R. pseudoumbilicus* (9.52%), *H. walbersdorfensis* (Supplement 1).

Rohožník (R)—new data were obtained from two samples of *Lithothamnion* limestone from Vajarská. R1 has impoverished diversity dominated by *R. minuta* (30.76%). R2 includes mainly *R. minuta* (12.5%) *T. milowii* (12.5%) with no index fossils (Supplement 1). Only poor nannoflora was mentioned in Hladilová et al. (1998).

Stupava–Vrchná hora (VH)—new data. Two nannofossil and five samples of foraminifera were analyzed. From VH1 *C. floridanus*, *Reticulofenestra* sp., *T. carinatus* were identified. Sample VH5 from *Lithothamnion* limestone consists only of long-ranging species *R. minuta* (43.47%), *C. pelagicus* (8.69%), *U. jafari* (8.69%) with no index fossil or zonal marker (Supplement 1).

Devínska Kobyla Hill (DK) and Sandberg (S) (Hyžný et al. 2012; Pivko et al. 2017; Ruman et al. 2017). However, 48 samples were analyzed by Hyžný et al. (2012), we used 11 of these samples (S1.1–1.4, S1, S2.1–2.6; Supplement 1). The main nannofossil assemblage composition

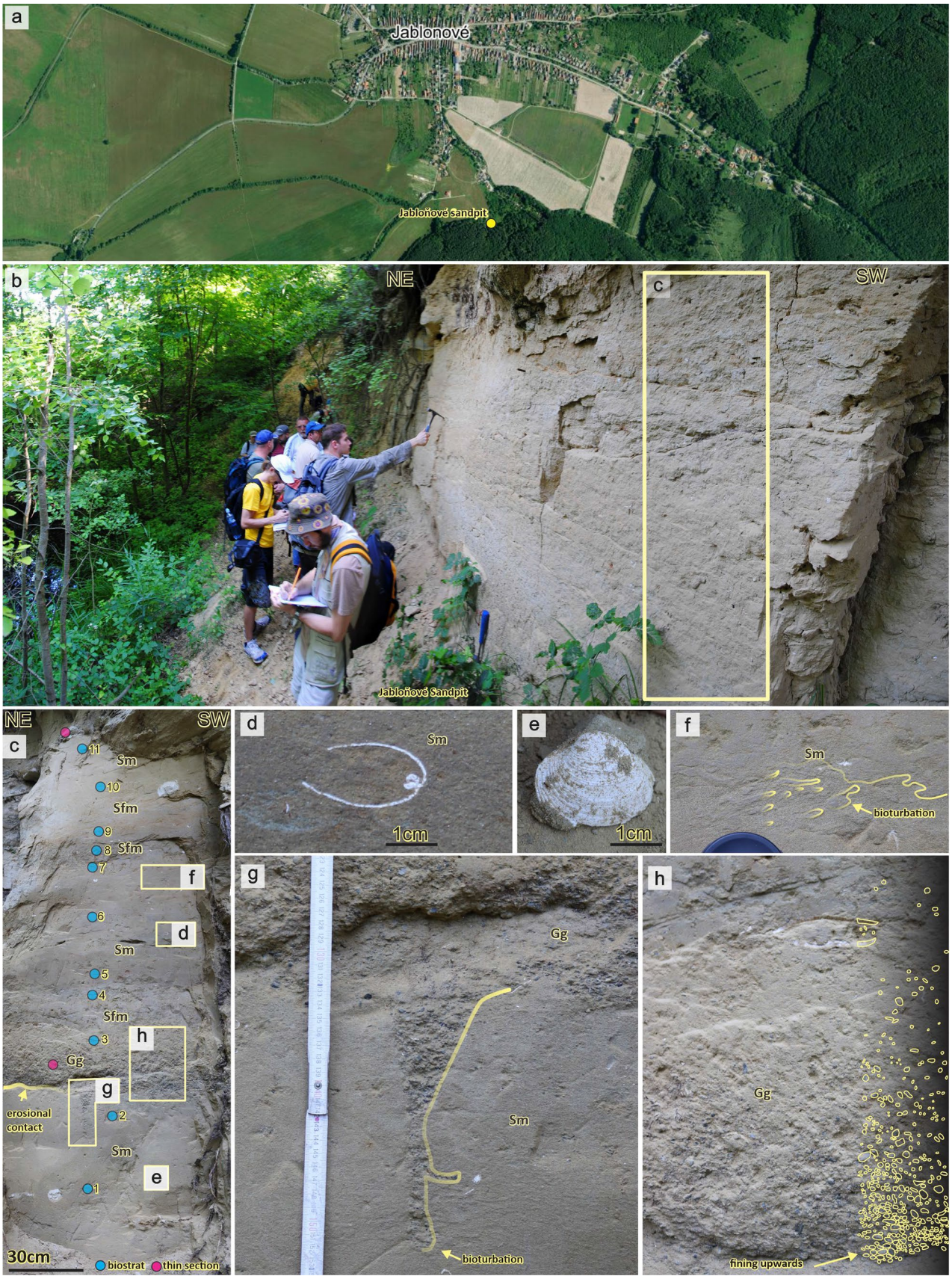
a
Jablonové
Jablonové sandpit
b
NE
Jablonové Sandpit
c
SW
NE
SW
11
Sm
10
Sfm
9
8
Sfm
7
f
6
d
Sm
5
4
Sfm
3
h
Gg
g
erosional contact
2
Sm
e
1
30cm
biostrat
thin section
d
Sm
1cm
e
1cm
f
Sm
bioturbation
g
Gg
Sm
bioturbation
h
Gg
fining upwards

◂**Fig. 4** Jabloňové sandpit studied profile. **a** Location map adopted from Google Earth Pro, Image © 2022; **b–h** section with facies descriptions and specific details; **d**, **e** Venerid bivalve. For explanatory notes on lithofacies, see Fig. 5

represents *C. pelagicus*, *C. floridanus*, *R. haqii*, *R. minuta*, *R. pseudoumbilicus*, and other age-supporting taxa *Calcidiscus macintyrei*, *C. premacintyrei*, *C. tropicus*, *H. carteri*, *H. wallichii*, *S. abies*, *U. jafari*.

Devínska Nová Ves tehelňa–DNV clay pit (D)—The calcareous nannoplankton list was adopted from Jamrich and Halásová (2010), with 69 samples analyzed. The main taxa are *C. pelagicus*, *R. haqii*, *R. minuta*, *R. pseudoumbilicus*, *B. b. parvula*, *H. wallichii*, *H. macroporus*, *R. sicca*, *S. abies*, *S. pulchra*.

Foraminifera

Seventeen samples (1–17) of benthic foraminifera from the **ZT** section were studied in detail. In total, 86 Neogene taxa were determined (Fig. 11). Preservation of foraminiferal tests is good to moderate. *Bulimina* species are most abundant in the entire profile (up to 90% in 4–7 and 17), followed by *Bolivina* (ca. 30% in 5–6), *Cassidulina* (up to 30–35% in 15, 12, 8, 5) and keeled elphidia (ca. 30% in 13, 3 and 1). Individuals of *Melonis* were well represented (up to 20%) in 16, 14, 10, 9, 2. Dimensions (width/length) of benthic foraminifera (770) with mass prevalence of elongated forms from samples 4, 5, and 6 were measured to reveal a possible taphonomic effect (Fig. 12, Supplements 2, 3c).

Cluster analysis based on the Bray Curtis similarity index shows three groups (A, C, D) and outlier (B) at the ca. 68 similarity level (Fig. 13a, Supplement 3d), similarly as shown by PCA and NMDS analyses (Figs. 13b, c).

From **BAZ**, two foraminifera samples were studied. BAZ1 from washed residue over 1 mm contains a lot of *Amphistegina* tests, Bryozoa, red algae, and crab claws. Most foraminifera tests are coated by coccolith-rich crusts (Fig. 11) and comprise 90% of the fine (0.071–1 mm) residue. The assemblage (SSD 22) contains common *Lobatula lobatula* (32%), *Cibicides* sp. div. (10%), *Biasterigerina planorbis* (17%) together with *Textularia pala*, *Cancris auricula*, *Elphidium fichtelianum*, *Reussella spinulosa*, and *Sphaerogypsina globulus*, rare infauna was badly preserved. Plankton includes *Globigerina bulloides*, *G. regularis*, and *Dentoglobigerina altispira*. Sample BAZ2 contained many mollusk shells, echinoderm fragments, Cirripedia, and fish bones. Foraminifers (SSD 20) are similar to BAZ1, the most abundant is *L. lobatula* (33%), with the umbilical part strongly affected by the shape of the substrate. The rare planktonic group contains mainly *G. bulloides* and *D. altispira* specimens. Small specimens of *Globocassidulina*, *Hansenisca*, and *Nonion* with different shell preservation are also present.

Eight samples from the **J** and **K** unveiled new data, two were barren. Sample J4 in fine-grained residuum contains a foraminifera-rich assemblage (SSD 21) dominated by *Ammonia inflata*, small non-keeled elphidiids as *Elphidium excavatum* and *P. granosum*, accompanied by rests of echinoids, shark teeth, and mollusks shell debris. The dominance of *A. inflata* (to 35%) is stable within the entire profile (Supplement 2). Species diversity values are from 8 (J10) to 24 (J4). **K** yields associations rich in *L. lobatula*, *Cibicides* sp., *T. pala*, and elphidiids (SSD 22).

Foraminifers from **VH** profiles are generally in coarser-grained residue, containing sharp-edged quartz and large mica crystals. Foraminiferal tests are poorly preserved, often with clasts stacked into the foraminiferal test complicating the determination of specimens. Foraminifers are scarce in samples 3, 4 were more abundant and consisted of well-preserved specimens dominated by *B. planorbis*, *E. crispum*, *E. rugosum*, *A. inflata*, *Guttulina austriaca*, *Globulina striata* (Supplement 2). Sample 5 is solid algal limestone, and foraminifers were studied in thin sections. Abundant *Borelis melo*, *Quinqueloculina*, *Triloculina*, *Amphistegina* sp. were identified.

NMDS analysis of the data matrix using Bray Curtis similarity (Fig. 14a) shows four distinct groups: the first group with low SSD dominated by epiphytic *Biasterigerina*, *Neoconorbina*, *Ammonia*; a second group with higher SSD dominated by epiphytes (*Lobatula*, *Amphistegina*, keeled elphidia), the third group of high diversified assemblages rich in *Melonis*, *Cassidulina*, flat *Bolivina* and *Uvigerina* and the fourth group dominated by *Bu. elongata*. Sheppard's diagram proves stress 0.1242, confirming the NMDS result's plausibility (Fig. 14b).

The new foraminiferal data of the late Badenian age were combined, analyzed, correlated, and evaluated with datasets from published results. The listing of additional results is in alphabetical order:

DK and **S** (Hyžný et al. 2012; Pivko et al. 2017; Ruman et al. 2017). In all studied samples from these localities, specimens of keeled elphidia are most abundant (exceeding 50%). The dominant species are *E. crispum* followed by *Neoconorbina terquemi*. The average species diversity of the studied assemblages is low (SSD 8–9). The Shannon_H and Fisher α diversity indices also reach very low values ($H = 0.5–2$; $F\alpha = 0.6–6.0$). The algal limestones or algal patches parts thin sections study show the prevalence of *Elphidium*, *Miniacina*, *Neoconorbina/Asterigerinata*, *B. melo*, and less porcellaneous forms such as *Quinqueloculina*. The most abundant coralline algal genus is *Mesophyllum*. *Lithothamnion*, *Lithophyllum*, and *Spongites* are less frequent, while thin encrustations of *Titanoderma* and *Hydrolithon* are rare (Pivko et al. 2017). In the algal limestones

Lithofacies code	Lithofacies	Sedimentary textures	Depositional process	Interpretation/paleobathymetry
Gg	Fossiliferous, bioturbated, matrix support, granule to pebble sized gravel with well sorted and rounded clasts	Normal gradation	Wave action or less likely uni-directional traction	Shoreface (0-6 m)
Sm	Fossiliferous bioturbated medium to fine grained sand, well sorted and rounded scarce plant fragments	Massive	Wave action	Inner Shelf (6-60 m)
Sfm	Fossiliferous bioturbated muddy sand, scarce plant fragments	Massive	Wave action	Inner Shelf (6-60 m)

Fig. 5 Jabloňové sandpit: lithofacies description and interpretation

from Merice locality (Hyžný et al. 2012; near *Lingula* bed), miliolid forms (*Quinqueloculina* sp. div., *Cycloforina contorta*, *Triloculina* cf. *tricarinata*, *Pseudotriloculina*) prevail.

D—The foraminifera list was adopted from Kováčová and Hudáčková (2009). The profile alternates between associations dominated by plankton or benthos; only in a few samples is an association rich in both components documented. Benthic foraminifera are dominated by *Pappina neudorfensis*, *Bolivina dilatata*, *Bulimina elongata*. Planktonic foraminifera consist of various forms of *G. bulloides* and *Turborotalita quinqueloba*. Diversity (DSS) varies from very low (2–4) to high (72–89) (Kováčová and Hudáčková 2009).

Rohožník (R) Konopiská—Foraminifera from pelitic sediments determined Badenian and Sarmatian age. Foraminifera lists (boreholes RV-42, RV-44, Čierna 1973), Hladilová et al. (1998) and Fuksi (2012, 2015) were used. The foraminiferal assemblage was also studied in Ruman and Hlavatá Hudáčková (2015), where it was described as rich in *Lobatula*, *Tretomphalus*, *Biasterigerina*, keeled elphidia, small miliolid taxa *Pseudotriloculina*, *Quinqueloculina*, and *Miliolina*. Planktonic foraminifers are rare, represented by *Globigerina*.

Rohožník (R) Vajarská locality in the old limestone quarry shows a rich algal assemblage (Schaleková 1973); we studied foraminifera from new thin sections from the outcrop. The two associations were recorded—one with a dominance of *L. lobatula*, *P. mediterranensis*, *Elphidium* sp., *Amphistegina* sp., and a second with *B. melo* and *Pseudotriloculina*, *Quinqueloculina*, *Miliolina*.

Stupava tehelňa (clay pit)—Boreholes 100–150 m deep were drilled to analyze municipal waste disposal conditions. The site was assigned to the *Bulimina–Bolivina* Zone. The foraminiferal association is very similar to the DNV clay pit upper part, dominated by *P. neudorfensis*, *B. dilatata*, *Bu. elongata* in the benthic association. Planktonic foraminifera consist of various forms of *G. bulloides* together with *T. quinqueloba* and *G. obesa*. For our study, we adopted the foraminifera list from the report by Šujan et al. (1992) and Hudáčková and Kováč (1993).

NMDS statistical analysis of all samples (Fig. 15a, Supplement 2) shows almost the same four groups of samples as in the ZT profile together with all newly studied samples. The first is represented in the D outcrop dominated by *Bulimina* and *Bolivina*, partly in R and ZT localities with a high portion of *Bu. elongata*. The second group is composed of highly diversified samples R, ZT, L, G sites with the main portion of *Melonis*, *Cassidulina*, *Globocassidulina*, *Uvigerina*, the third group contains J, K, S, R, BAZ, VH, and F sites (SSD 5–20) with the prevalence of *Lobatula*, *Amphistegina*, keeled elphidia, *Ammonia* (Supplement 2). Sheppard's diagram proves stress 0.197, which represents good plausibility (Fig. 15b). Principal component analysis (Fig. 16) shows five components explaining ca. 75% of variability representing original variables (the most significant species) influenced deployment of associations. The highest negative PC1 (variation in the data) component score represents flat smooth *Bolivina* (– 0.738), and PC2 with *Uvigerina* sp. div. (– 0.3414), *Bu.* ex. gr. *elongata* (– 0.2663), while the highest positive eigenvalues reach keeled elphidia (0.432) and *Biasterigerina* (0.169).

Palynology

Thirteen samples (Fig. 17) from ZT (4–12 and 14–17) were processed for pollen and palynofacies analysis. Samples 4, 6, 7 represent the most diversified pollen assemblage. Sample 5 has remarkably well-preserved palynomorphs but differs in palynofacies type–dominancy of Pinaceae (Supplement 4).

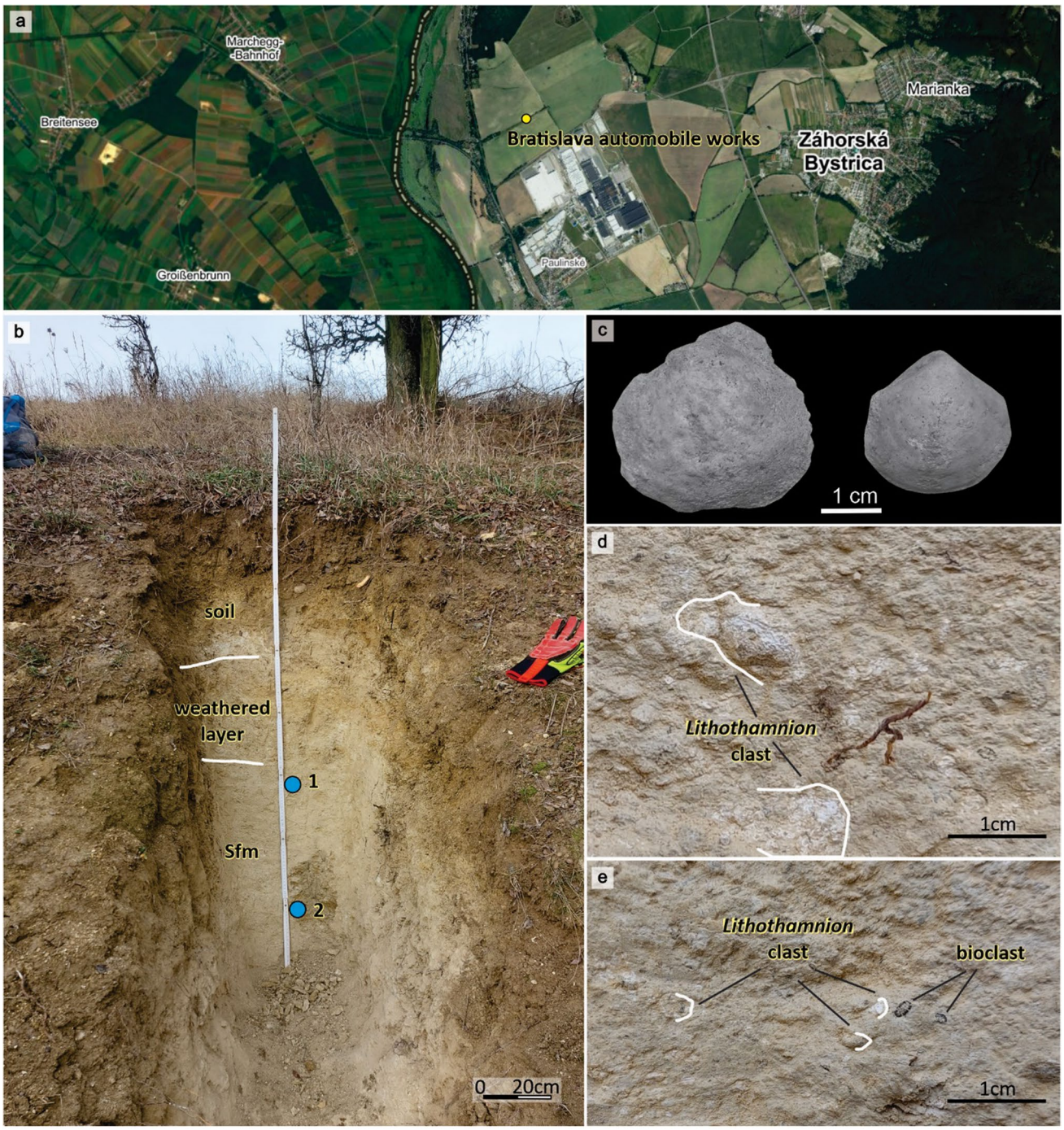

f

Lithofacies code	Lithofacies	Sedimentary textures	Interpretation/paleobathymetry
Sfm	Bioturbated,fossiliferous sandy-mudstone with *Lithothamnion* clasts	Massive	Shelf

Fig. 6 BAZ (Bratislava automobile works) studied section. **a** Location map adopted from Google Earth Pro, Image © 2022; **b, d, e, f** detailed sections with facies descriptions/interpretations and specific details of *Lithothamnion* and bioclasts; **c** articulated bivalve casts

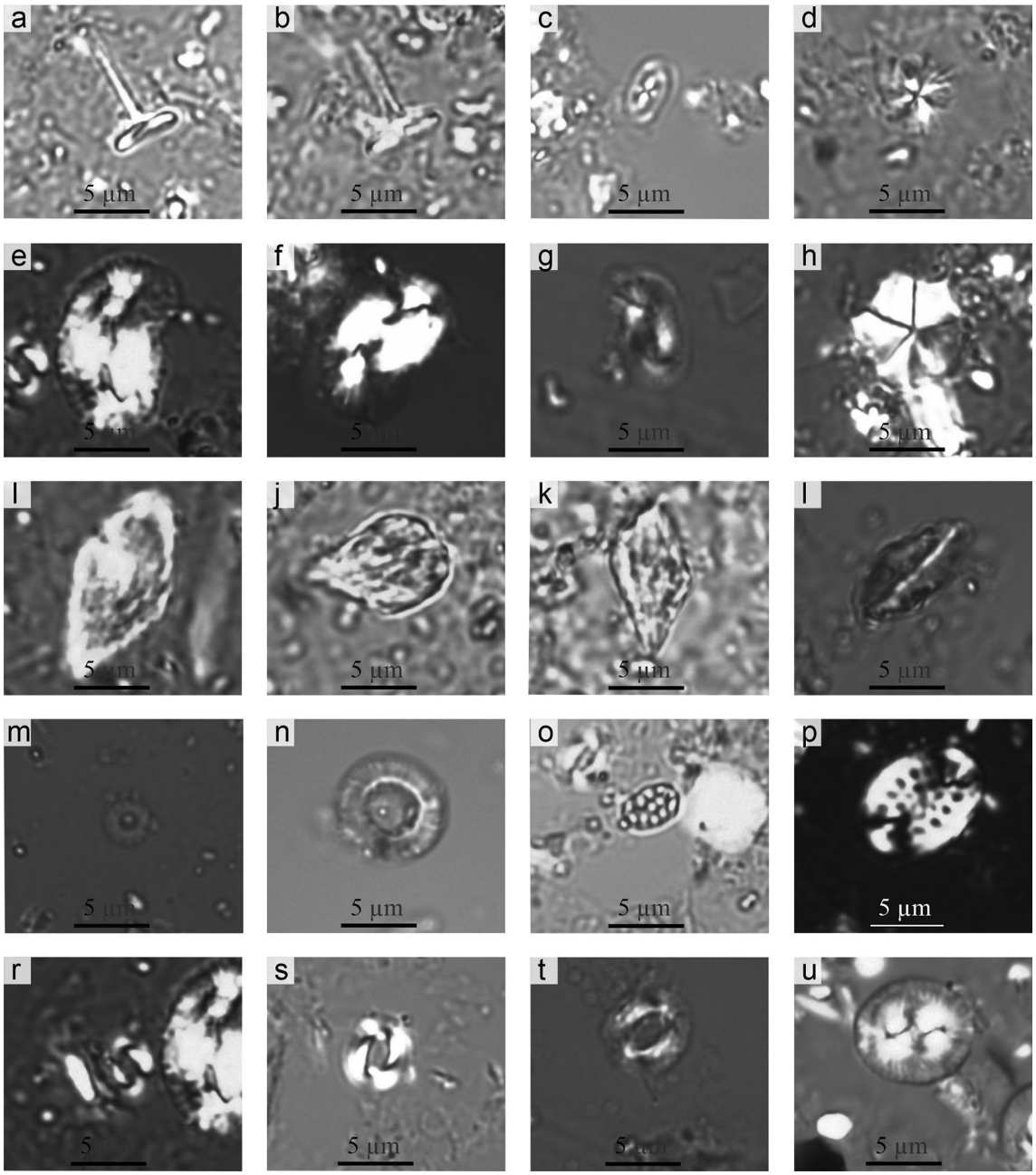

Fig. 7 Calcareous nannofossils. **a, b** *Rhabdosphaera sicca*, ZT5, ZT17; **c** *Syracosphaera pulchra*, ZT5; **d** *Sphenolithus abies*, ZT8; **e, f** *Helicosphaera wallichii*, ZT5, ZT11; **g** *Helicosphaera carteri*, J4; **h** *Braarudosphaera bigelowii parvula*, ZT10; **i** *Triquetrorhabdulus milowii*, ZT8; **j–l** *Orthorhabdus rugosus*, ZT9, ZT11, J9; **m** *Umbilicosphaera jafari*, BAZ1; **n** *Umbilicosphaera rotula*, ZT9; **o** *Holodiscolithus macroporus*, ZT9; **p** *Pontosphaera multipora*, ZT5; **r** *Reticulofenestra haqii*, ZT5; **s, t** *Reticulofenestra pseudoumbilicus*, ZT8, J4; **u** *Coccolithus pelagicus*, ZT9

Interpretations

Sedimentary facies

ZT: A high concentration of thick-shelled bivalves, such as *Glossus humanus*, and increased bioturbation levels (**Sfl/Sfm** and **Fm**) suggest a medium to high-energy environment dominated by tide and/or wave action in the shoreface to inner shelf zone (Fig. 3). This environment was affected by an incision (scour fill) caused by matrix-supported conglomerates (**Gm**) with poorly sorted angular clasts. This indicates gravity transport by debris flows, which could have been

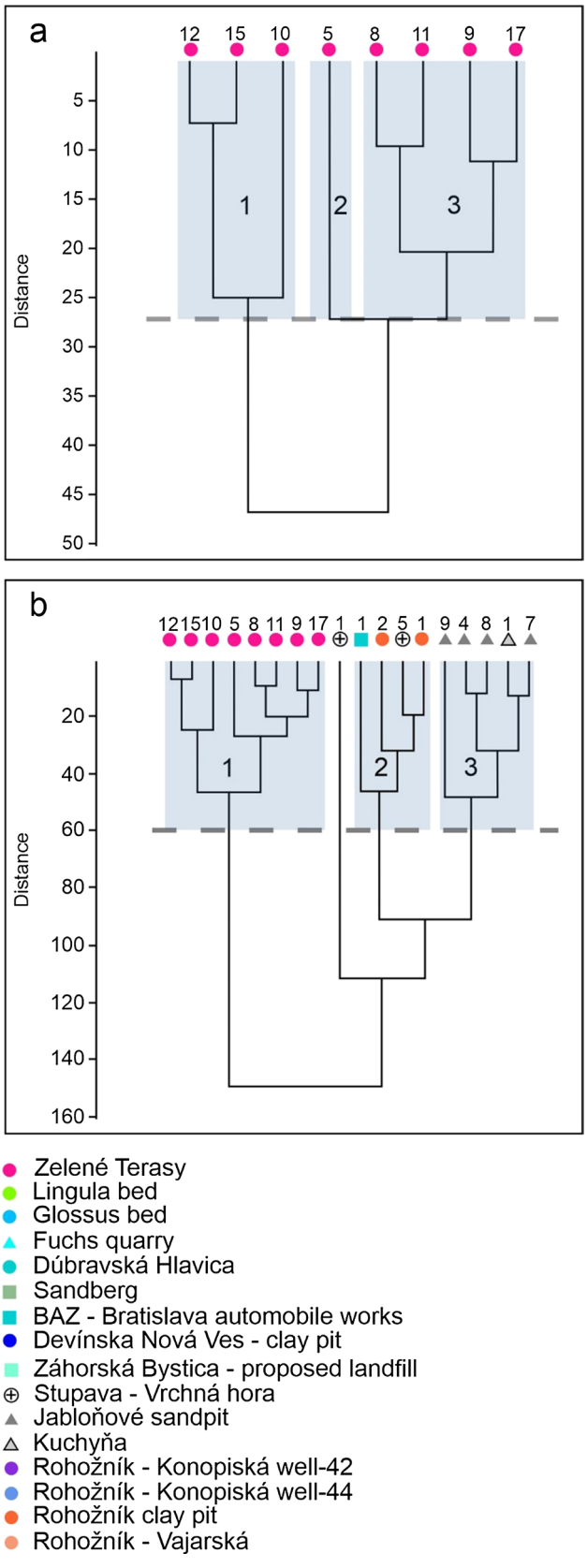

Fig. 8 Cluster analysis (Ward's method from percentages). **a** Zelené terasy (ZT) solely; **b** all newly studied sites including ZT (Supplement 3a, b). Explanatory notes: 1, 2, 3 = individual clusters, and locality symbols apply for all figures

triggered during a sea-level fall. The emerged area is likely associated with a coastal plain.

J: Well-sorted sands (**Sm, Sfm**) and conglomerates (**Gg**) in Figs. 4h and 5 indicate wave activity from the shoreface to the inner shelf. The observed high-intensity bioturbation aligns with Rossi et al. (2017), suggesting such patterns often reflect shallow marine conditions influenced by waves. Their findings, which emphasize well-rounded sediment grains and few coal fragments, match our observations in the **Gg** facies (Fig. 4h). The marine bivalves venerids and hiatellids, prevalent in all studied beds (**Sm, Sfm, Gg**), hint at a shallow marine environment. These bivalves are typically found in high-energy, shallow waters, as stated by Stanley (1970) and Pratt and Campbell (1956). While the erosional surface at the **Gg** facies base does not solely denote a coastal environment, its association with the normally graded conglomerate (**Gg**) suggests wave-induced dynamics. Rossi et al. (2017) confirm that such graded bedding, especially with marine fauna, often results from wave action, pointing to a coastal environment.

BAZ: The abundance of well-rounded *Lithothamnion* and other marine bioclasts embedded in the sandy mudstones (**Sfm**) indicates the presence of the shelf zone (Fig. 6).

Biostratigraphy and paleoecology (nannoplankton, foraminifera)

Biostratigraphy depends on nannoplankton and foraminifera. The nannoplankton zone was assigned to the presence of *O. rugosus* in this study (ZT9–12, 17, J9), whose first occurrence (FO) is generally considered as at the base of NN6 (Young 1998; Young et al. 2017). Other age-supporting taxa in the studied material include *B. b. parvula*, *H. wallichii*, *R. sicca*, *S. abies*, *U. jafari*, *U. rotula*. The studied assemblage is, therefore, assigned to NN6 Zone (Martini 1971). Higher numbers of *H. macroporus*, mainly from ZT and K samples, as previously mentioned from the D site, support the late Badenian age (Jamrich and Halásová 2010). Foraminiferal CPN9 Zone (Central Paratethys Neogene Zonation; Cicha et al. 1975) is given based on the occurrence of *P. neudorfensis* and *B. maxima* (ZT, D, BAZ, J, R). Rich plankton assemblage dominated by *Globigerina* sp. div. is present only in the D, S, R, JV samples. Rare *Orbulina universa* documents late Badenian age in the D and R samples and an $^{87}Sr/^{86}Sr$ age of 13.54 Ma (13.39–13.7 Ma) published by Hudáčková et al. (2003).

The most detailed paleoecological analyses have been done for ZT nannoplankton assemblages (Figs. 3, 7, 11)

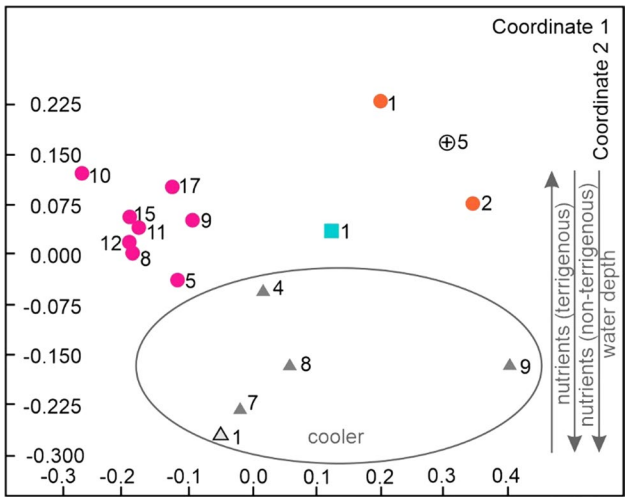

Fig. 9 Non-metric multidimensional scaling (NMDS) analysis (Bray Curtis from percentages). For explanatory notes, see Fig. 8

with common *R. haqii*, followed by *C. pelagicus*, indicating a nearshore nutrient-rich environment. Higher values of *R. haqii*/*C. pelagicus* ratio (Supplement 1) point to warmer stratified (stressed) waters with reduced upwelling (Báldi-Béke 1984; Andreeva-Grigorovich 1998; Auer et al. 2014; Ivančič et al. 2018). Associations from ZT10, 12, 15 (Fig. 8a) generally dominate along continental margins, indicating a strong influx of terrigenous material and relative proximity to the shore (Haq 1980; Aubry 1992). An influx of terrigenous material mixed with freshwater (brackish—*B. b. bigelowii*) may have resulted in the reworking of older taxa (sensu Ćorić and Hohenegger 2008; Auer et al. 2014). Association in ZT5 is equitable and transitional toward the third cluster (Fig. 8a). Cluster 3 with *H. macroporus* and low values of sphenoliths and rare discoasters indicate a cooling trend (Perch-Nielsen 1985; Lehotayová 1989; Spezzaferri and Ćorić 2001).

The correlation of nannofossil assemblages from localities along Malé Karpaty Mts. (ZT, J, K, BAZ, VH, R) shows variability in its origin. Small- and medium-sized reticulofenestrids dominate ZT samples (Fig. 8b) with higher SSD (Supplement 1) reflecting temperate water with nutrients derived from the coast. In contrast, cluster 3 with J and K with the prevalence of *C. pelagicus* reflects nutrient-rich stable upwelling waters (Cachão and Moita 2000; Jamrich and Halásová 2010; Auer et al. 2014). Cluster 2 (Fig. 8b) with BAZ, R1, R2, VH5 documents less nutrient-warmer conditions which is in accordance with NMDS analysis (Fig. 9). PCA biplot analysis (Fig. 10b) from the combined dataset, together with published data (Jamrich and Halásová 2010; Hyžný et al. 2012), shows the most decisive influence within samples (most of D, ZT10, S1-1) by *R. haqii* reflecting a more open sea, stress environment conditions. The associations of S, ZT5, 8, 12, J, K, D are dominated by *C. pelagicus*, reflecting cold waters and upwelling. Increased availability of terrigenous nutrients and stable water conditions (Haq 1980; Cachão and Moita 2000; Wade and Bown 2006; Ćorić and Hohenegger 2008; Auer et al. 2014) with prevalence of *R. minuta* (D, ZT9, 11, 15, 17, J, BAZ, VH, R) indicate warm water (Rahman and Roth 1990). NMDS analysis of this dataset proves equal distribution of the studied assemblages (Fig. 10a).

The obtained results are tied to paleogeography (Fig. 18) from the Devínska Kobyla Hill to Rohožník. The paleoenvironment of the Devín area (DSi, DZ, ZT, L, G, MQ) is interpreted as a bay-lagoon system. Water temperature varies from warmer stratified or mixed temperate to cooler depending on the currents. Terrigenous input and upwelling currents are the primary sources of nutrients. Thepaleoenvironment of the Sandberg area (lower part with massive bioturbated sandstone facies; Sm; Fig. 2) indicates shallow marine conditions under fairweather wave base but still with higher energy with normal salinity, warmer waters than mid-outer shelf upwelling influenced mudstones. The lower sequence passes into a low-energy environment Sfm in the upper part. The uppermost part of the limestone facies is characterized by corallinacean limestones representing a change in the sedimentation. Warm water nutrient tolerant *C. macintyrei*, *Discoaster variabilis*, *H. carteri*, *H. wallichii*, *U. jafari*, *S. abies* are documented in Sm and Sfm facies. Algal limestone facies yield a low diversified cosmopolitan nannoplankton, possibly due to low nutrient supply. The scarcity of planktonic foraminifers is caused by coast proximity.

Distally, temperate deeper waters with cooler episodes in D are supported by nannoplankton (*H. macroporus*) and foraminifera. Mass occurrence of *G. bulloides* and *T. quinqueloba* (D, ZB) documents temperate and cold water (Hilbrecht 1996) that rapidly responds to an increase in nutrient supply (Reynolds and Thunell 1985). Nearshore affinity and warmer indices (*D. altispira*) are documented only in the BAZ, coinciding well with the dominance of reticulofenestrids. Northeastwards located VH shows a nearshore environment as mentioned from S, with limestone facies. Further north, a different nearshore paleoenvironment is at J and K (Sm and Sfm facies), documented on the prevalence of *C. pelagicus* and *Globigerina* sp. div. reflecting cooler eutrophic and upwelling conditions. The most northeast sites are RV and RK. Limestone facies present in RV is similar to S. From RK (Fm facies), a rich plankton assemblage with *T. trilobus* and *O. universa* documents temperate warm waters further away from the coast.

The detailed analysis from the Devín area (DZ, ZT, L, G) reveals (1) well-oxygenated, euryhaline shallow (e.g., inner, mid-outer shelf) normal marine water conditions, (2) deeper normal marine (e.g., shelf-break slope) water with reduced

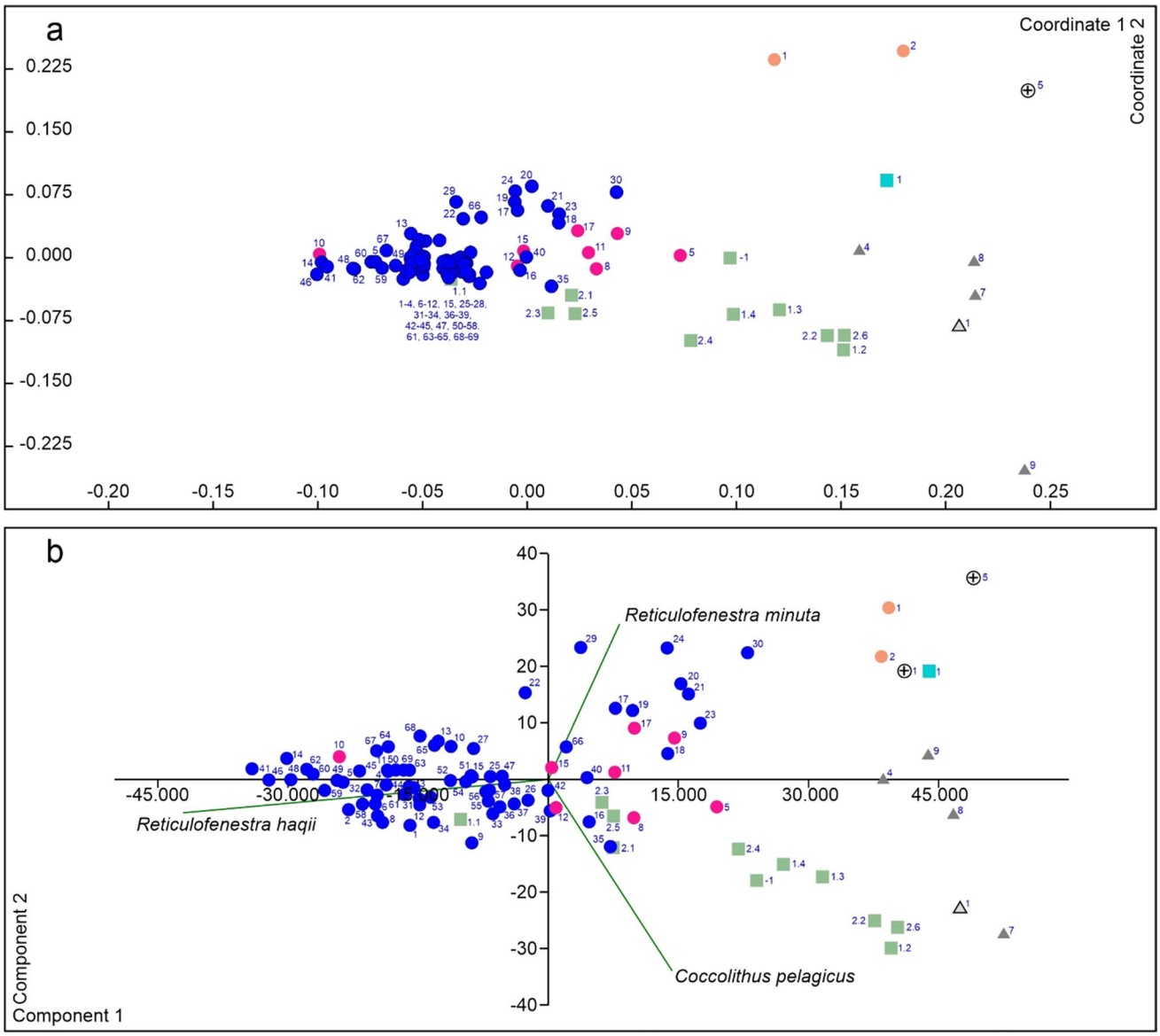

Fig. 10 **a** NMDS (Bray Curtis from percentages) analysis of the nannofossil association; **b** principal component analysis (PCA) biplot analysis of all localities with dominant taxa expressed by green lines (including published results from DNV clay pit and Sandberg; Jamrich and Halásová 2010; Hyžný et al. 2012). For explanatory notes, see Fig. 8

oxygen content on the seafloor (Fig. 18a), (3) eutrophic normal marine deeper waters (e.g., shelf-break slope).

In the upper part of the ZT I profile (Figs. 2, 3, 18a), an autochthonous mass abundance of *Bu. elongata* (Figs. 11, 12, Supplement 2), usually indicating deep-water conditions (Fontanier et al. 2002), is here preserved in a generally shallow water (Švagrovský 1981; Hyžný et al. 2012) paleoenvironment depleted in oxygen (Kaiho 1994; Báldi and Hohenegger 2008; Kranner et al. 2021b). Cimerman et al. (1988) document the mass occurrence of *Bulimina* in shallow water conditions (water depth ca. 42 m) with low oxygen like the ZT I profile.

Dysoxic conditions in the Devín area are supported by *Varicorbula gibba*, which thrives well under such conditions and is present in ZT, DZ, G (Hyžný et al. 2012). *Varicorbula* is a typical opportunistic colonizer of disrupted habitats with a reduced number of accompanying taxa, which can quickly become a dominant faunal element (Hoffman 1977, 1979; Mandic and Harzhauser 2003). It is usually distributed from low intertidal zones to considerable depths of several hundred meters (Švagrovský 1981; Salas 1996). Significant abundances of *V. gibba* in subtidal muds in the northern parts of the VB could point to unstable conditions (Mandic and Harzhauser 2003; Fuksi et al. 2016; Soliman et al. 2023). A strongly stratified water column in the system of

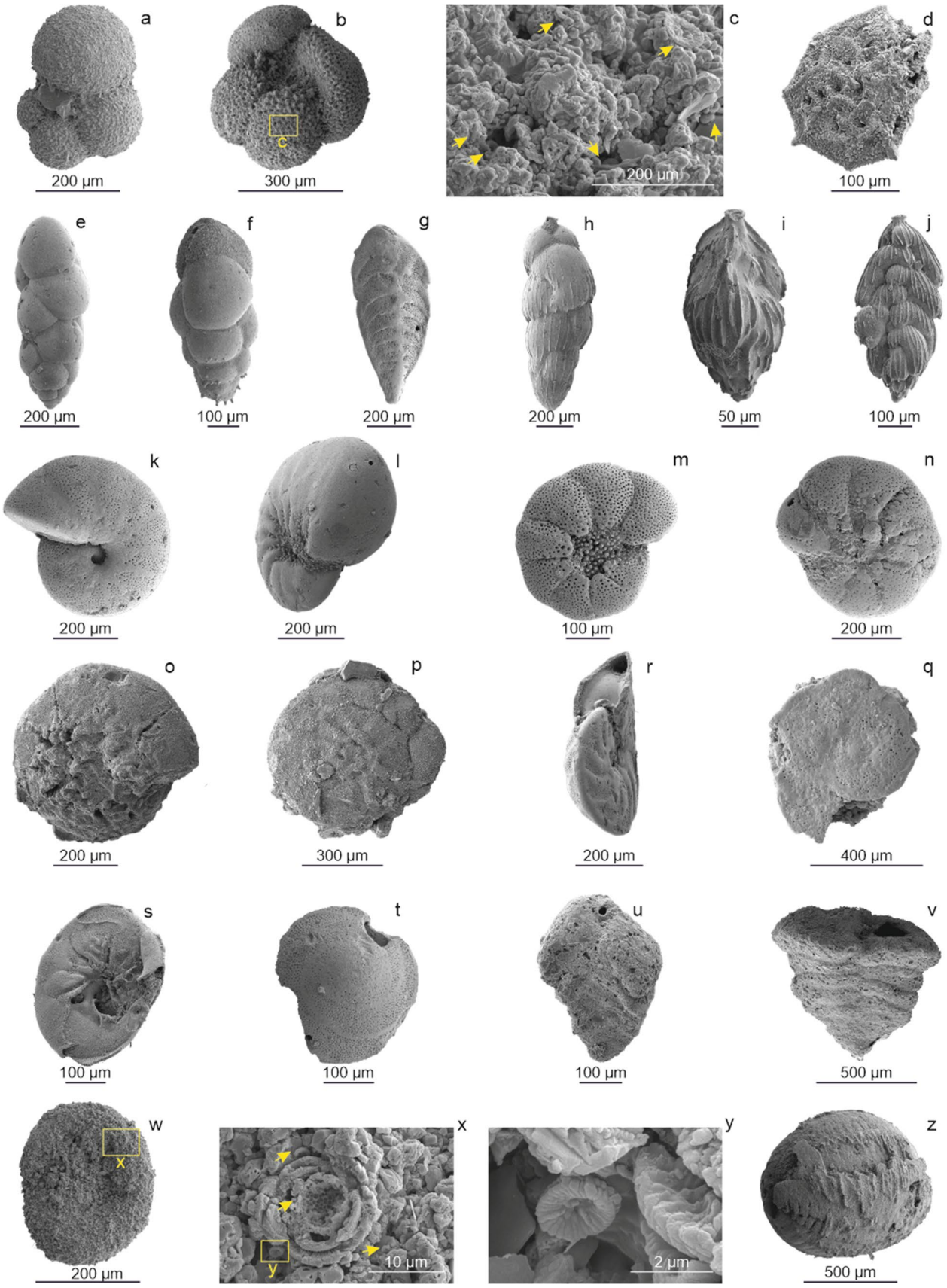
a
200 µm
b
c
300 µm
c
200 µm
d
100 µm
e
200 µm
f
100 µm
g
200 µm
h
200 µm
i
50 µm
j
100 µm
k
200 µm
l
200 µm
m
100 µm
n
200 µm
o
200 µm
p
300 µm
r
200 µm
q
400 µm
s
100 µm
t
100 µm
u
100 µm
v
500 µm
w
x
200 µm
x
y
10 µm
y
2 µm
z
500 µm

◂**Fig. 11** Foraminifera. **a** *Globigerinella obesa*, BAZ; **b** *Dentoglobigerina altispira*, BAZ; **c** *D. altispira* wall detail, focused on the crust covered with the nannofossils, yellow arrows show coccoliths, BAZ; **d** *Elphidium josephinum*, ZT; **e** *Bulimina elongata*, ZT; **f** *Bulimina subulata*, ZT; **g** *Bolivina maxima*, ZT; **h** *Uvigerina semiornata*, ZT; **i** *Trifarina bradyi*, ZT; **j** *Pappina parkeri*, ZT; **k** *Melonis pompilioides*, ZT; **l** *Nonion commune*, ZT; **m** *Porosononion granosum*, ZT; **n** *Porosononion granosum*, VH; **o** *Ammonia inflata* umbilical side, J; **p** *Ammonia inflata* spiral side, J; **q** *Lobatula lobatula* umbilical view, VH; **r** *Lobatula lobatula* apertural view, ZT; **s** *Biasterigerina planorbis* umbilical view, K; **t** *Biasterigerina planorbis* spiral view, K; **u** *Textularia gramen*, ZT; **v** *Textularia pala* apertural view, J; **w** *Rosalina obtusa* umbilical view, BAZ; **x** *R. obtusa* wall detail, focused on crust of the nannoplankton coccolith, yellow arrows show coccoliths, BAZ; **y** *R. obtusa* wall detail, focused on crust with coccolith, BAZ; **z** *Borelis melo*, VH

narrow channels and protected lagoons can be the reason for the emergence of such communities. A shallow water shelf environment with increased temperatures, and thus also salinity increase will enable the seawater to be supersaturated by CO_3^{2-} (Morse et al. 2007), leading to calcium carbonate precipitation. Such conditions are supported by the dominance of *Amphistegina*, which is associated with algal limestones (Hallock 1985) visible in ZT, L, S, J, K, RV. Well-aerated oligotrophic shallow water with seagrass or rigid substrate suitable for algal patch reef growing is observed in upper Badenian strata today exposed on the Malé Karpaty Mts. slopes (S, F, VH, K, J, RV). Algal limestone with *Lithothamnion* remnants in life position is documented in S, RV, VH (Schaleková 1969, 1973; Hrabovský and Fordinál 2013; Pivko et al. 2017) and in the ZT, BAZ, J the algal limestone clasts are also present (this study; Figs. 3, 4, 6, 19). Coccolith crusts document an oligotrophic environment and low terrigenous input on foraminifera tests from BAZ (Fig. 11). A similar situation but with high productivity is mentioned by Vlček et al. (2022).

Significant change in the sediment is documented by benthic assemblage, which varies from mud–silty mud, sand, to limestone. A muddy bed is documented by infaunal genera such as *Bolivina* and *Bulimina*, together with *Melonis* in the westernmost part of the Devínska Kobyla slopes (DZ, ZT, G) and D, Záhorská Bystrica (JV) situated further from the seashore. Sandy seabed covered by seagrass is documented by the prevalence of epiphytic taxa such as *Biasterigerina*, *Amphistegina*, and keeled elphidia in the localities nowadays in a higher position on the foothills of Devínska Kobyla and Malé Karpaty Mts. (L, FL, S, K, J). Algae reef (carpets and patches) was identified based on the algae buildups and abundant miliolids (*B. melo*) at various localities from Devínska Kobyla—S, VH, R (Fig. 19). Apart from changes in substrate type, there were also changes in oxygen level and nutrient supply. Low oxygen levels correlate well with fine, muddy sediment, especially in open sea environments identified from D, ZB, RK in nowadays different positions. We have identified former bays (Fig. 18a) on the western slopes and central part of Devínska Kobyla Hill (G, ZT, L) with a low oxic and cold-water environment in the shallow water sediment on the presence of *Bulimina–Bolivina* together with *C. laevigata* associations. Stratified water column with freshwater input is indicated by warmer and lower salinity tolerant taxa *B. bigelowii* (Bartol et al. 2008), small reticulofenestrids from ZT and G together with the absence of planktonic foraminifera.

Palynology

Palynology analysis of the studied area shows different coastal vegetation types. Samples ZT4, ZT6, ZT7 reflect an almost marginal depositional environment, shallow water with local swamps, and diversified terrestrial pollen flora (Supplement 4). The zonal vegetation elements indicate a humid subtropical climate. Very good preservation of palynomorphs indicates dysoxic conditions in the depositional system. Well-preserved marine palynomorphs occur in ZT5 and ZT11. Samples ZT8–10, ZT12, ZT14–16 reflect an oxic environment or taphonomic processes that led to the degradation of organic matter and reflect environmental dynamics, such as mechanical damage and sorting or the original size of the clasts. The association from D is dominated by Pinaceae and Fagaceae, what represents riparian forests and swamps together with extrazonal mountain vegetation (Supplement 4). Zonal vegetation reflects subtropical to warm-temperate humid climate. S, BAZ, ZB, VH were barren of palynofossils due to unfavorable conditions of the coastal sediments (Sm facies).

Data from the upper part of ZT profile (ZT4–6) can be correlated with data published by Sitár and Kováčová-Slamková (1999). The dinoflagellate cysts assemblage from ZT correlates well with the upper Badenian association described by Soliman et al. (2023) reflecting marine, tropical to warm-temperate climate conditions.

Discussion

Four distinct, genetically diverse lithofacies delineate the upper Badenian paleoenvironments of the VB eastern margins (Slovakia). While these lithofacies are widely recognized, they have yet to be comprehensively described and defined individually. In the Slovak part of the VB, the Studienka Fm. is characterized by massive to laminated mudstones, indicative of a mid-outer shelf to deep basin setting. This facies is also evident in archived data (Čierna 1973; Šujan et al. 1992; Hudáčková and Kováč 1993; Kováčová and Hudáčková 2009; Jamrich and Halásová 2010; Fuksi 2012). Support for the deep-water nature of this facies comes from seismic reflection data, which reveals prograding

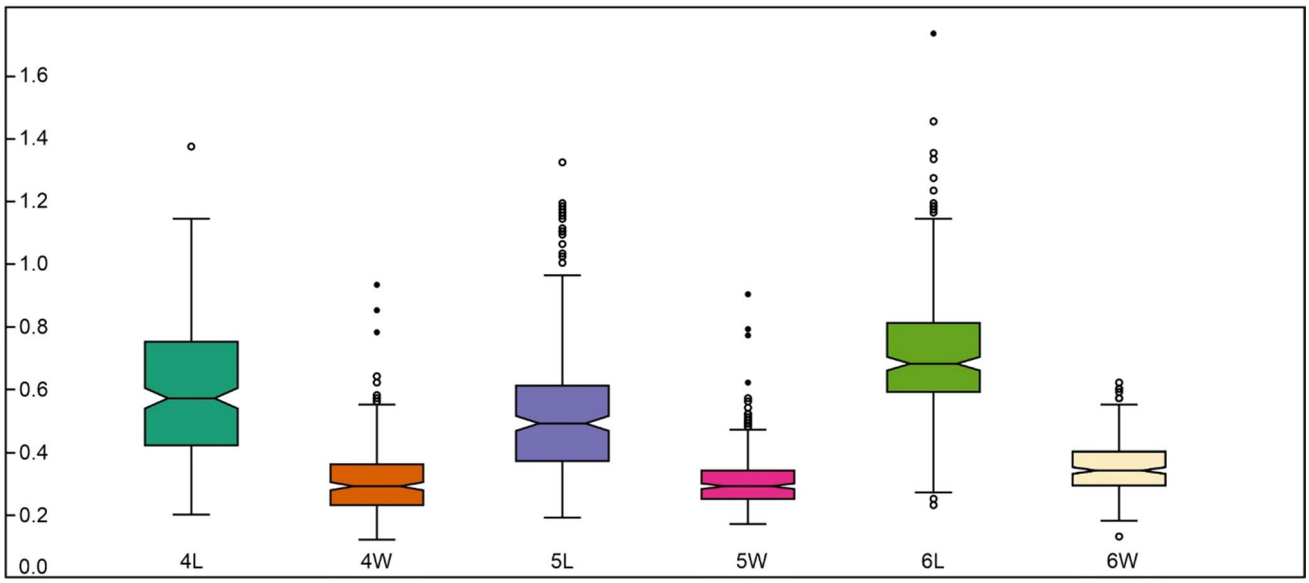

Fig. 12 Boxplots illustrating benthic foraminifera width/length ratio with mass dominance of elongated forms (ZT4, 5, 6), documents wide size shell variability without size sorting (Supplement 3c)

oblique clinoforms that are hundreds of meters thick (Kováč et al. 2004; Paulissen and Luthi 2010; Paulissen et al. 2011; Lee and Wagreich 2017; Kranner et al. 2021a; Csibri et al. 2022). Based on the classification scheme by Pellegrini et al. (2020), these clinoforms can be categorized as part of the shelf-break slope environment. In the Austrian part of the basin, this facies is referred to as the Rabensburg Fm. (Harzhauser et al. 2020). Described facies exhibit a lateral transition to massive muddy and sandy facies with a ~ 3:1 ratio, as identified by this and previous studies (e.g., Kováčová and Hudáčková 2009; Fordinál et al. 2012; Hyžný et al. 2012). These sediments have been classified as deep basin facies up to fossiliferous mudflats and lagoons (Harzhauser et al. 2020), correlating with outer to inner shelf settings. Examples of these facies can be found in the present study, specifically at the Zelené terasy I, III, IV and in numerous archived studies describing sections and shallow wells at the eastern VB margin (Fordinál et al. 2012). Meanwhile the shallow water facies are still commonly referred to as the Studienka or Rabensburg fms. (Harzhauser et al. 2020; Harzhauser 2022a, b, c; Kranner et al. 2021a), it is recommended that the shallow water facies should be defined as separate member or formations due to their distinct genetic environment.

The shallow water muddy facies may be transitional to facies dominated by sands, featuring uni-directional (Březina et al. 2021) to bi-directional (Ruman et al. 2017) cross-beds and clinostratified, unsorted conglomerate bodies (Nehyba and Roetzel 2004; Baráth 2009). These facies are associated with alternating terrestrial (fluvial and alluvial fans) and shallow marine environments (wave and tide-dominated coast) (Pivko et al. 2017; Ruman et al. 2017). The sandy facies might exhibit heavy bioturbation, which is so pronounced that the primary structures are disintegrated, which results in their massive appearance. Such facies have been documented in this study, for example, at the Jabloňové sandpit, as well as in archived studies from the Devínska Kobyla Hill (Hyžný et al. 2012). Both marine and terrestrial macrofauna are found, including the famous remains of hominids (Holec and Emry 2003). Baráth (1993) proposed a separate member within the Studienka Fm. for these facies, referred to as the Sandberg Mb.

However, the issue arises because the member includes mudstones, sandstones, conglomerates, and limestones. To avoid conflicts with the nomenclature, defining two genetically different shallow water upper Badenian fms. is essential (lateral equivalents of Studienka/Rabensburg Fm.): 1 clastic Stupava Fm., 2 limestone Sandberg Fm.

Definition of the **Stupava Formation**:

Derivation of name: Named after the town near Bratislava, "Stupava town."

Synonyms: Stupava Mb.; Láb *Amphistegina* sands (horizon) (Fordinál et al. 2012; Hrabovský and Fordinál 2013).

Type section: The peak of Vrchná hora Hill, located near Stupava (48°15′39.34″ N, 17° 2′48.39″ E) is in the VB, Záhorie lowland, Slovakia. The site placed SE of Stupava above the gardening area was initially referenced by Fordinál et al. (2012) and was subsequently described in greater detail by Hrabovský and Fordinál (2013).

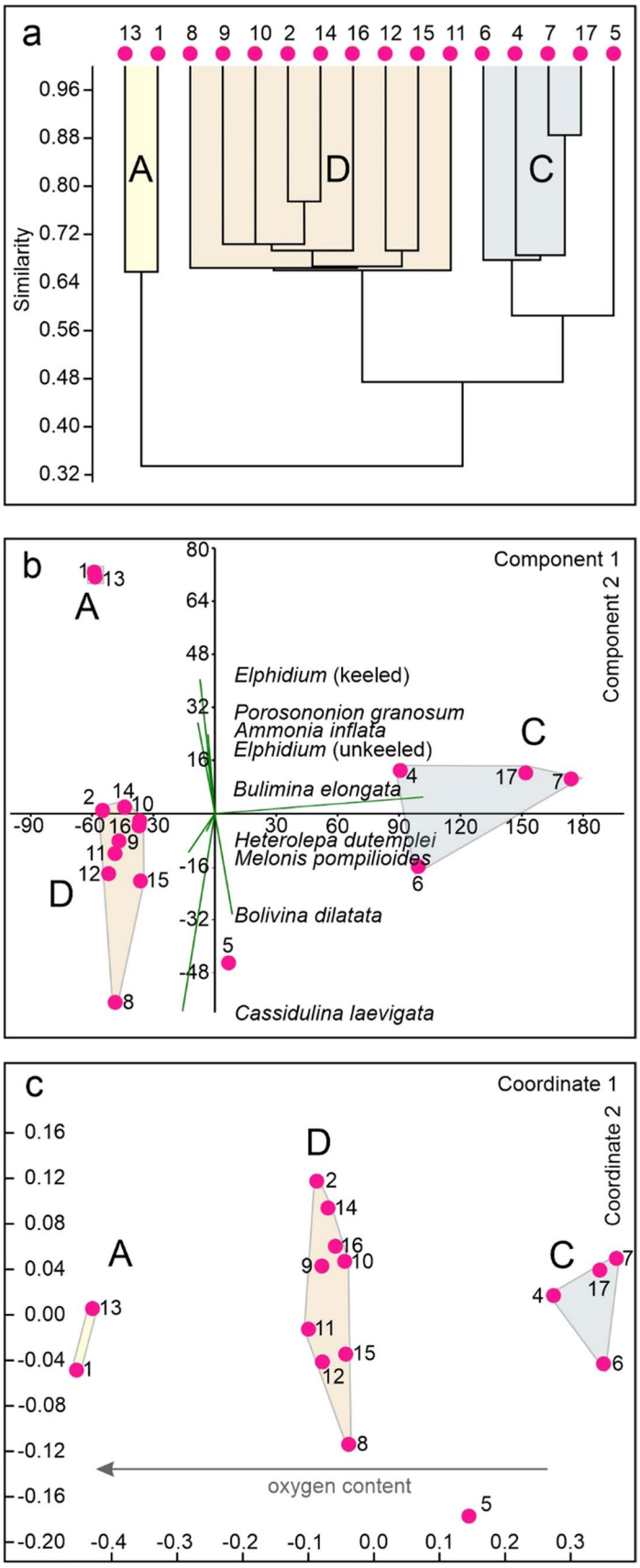

Fig. 13 Statistical analyses of the foraminifera association (ZT locality). **a** Cluster analysis (Ward`s method from percentages) shows three groups A dominated by *Ammonia*/*Elphidium* genera, C dominated by *Bulimina*/*Bolivina*, D grouped highly diversified samples (Supplement 3d); **b** Shows same groups resulted from PCA biplot with dominant taxa expressed by green lines; **c** NMDS (Bray Curtis from percentages) with oxygen content as a main discriminant

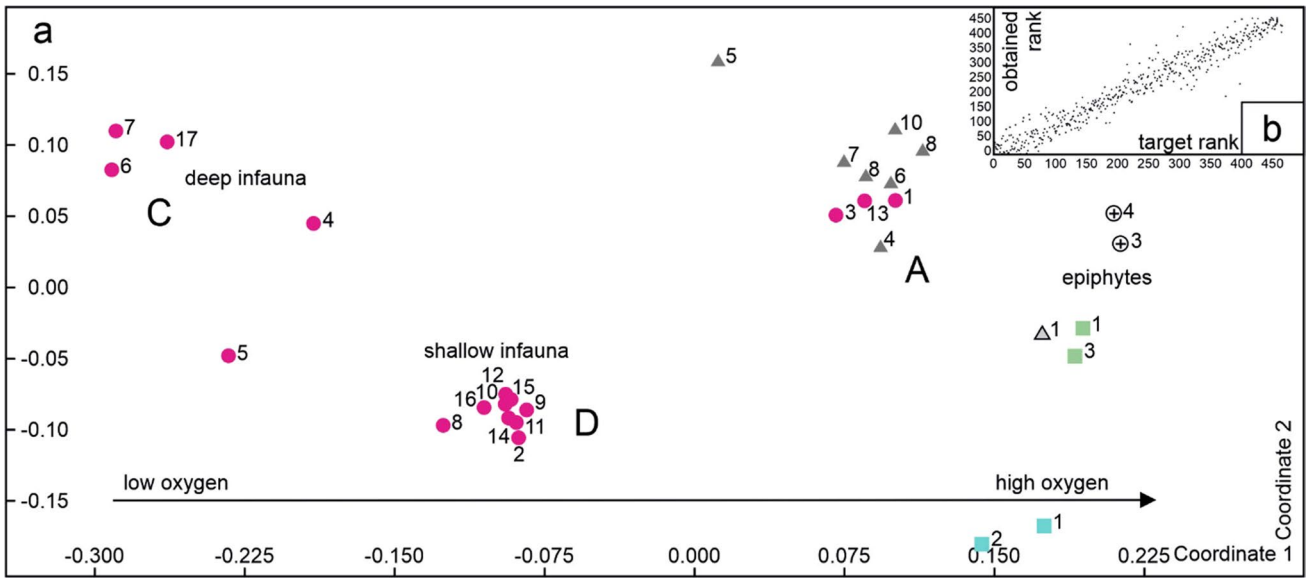

Fig. 14 **A** NMDS (Bray Curtis similarity) of the newly obtained foraminifera associations; **b** Sheppard's diagram of the foraminifera associations. For explanatory notes, see Fig. 8

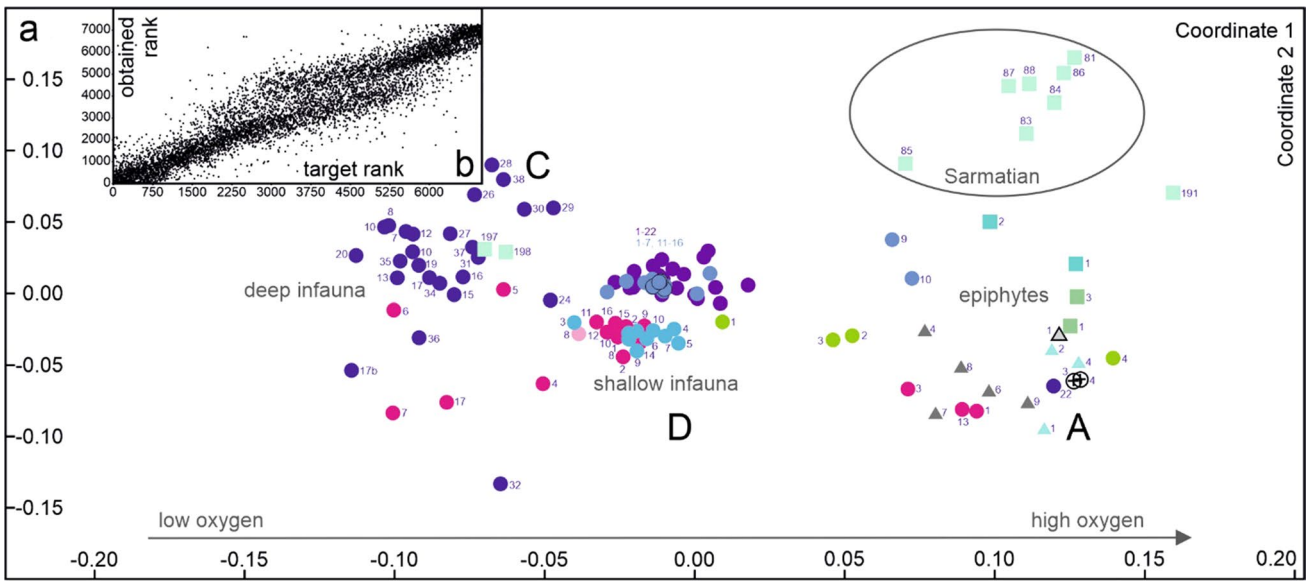

Fig. 15 **a** NMDS (Bray Curtis similarity) of the foraminifera associations entire dataset (new and published data); **b** Sheppard's diagram of the foraminifera associations. For explanatory notes, see Fig. 8

Thickness: The thickness spans several tens of meters, as corroborated by multiple composite outcrops scattered around the hill`s summit (Hrabovský and Fordinál 2013).

Lithology: The Stupava Fm. is characterized by the abundance of massive sands and sandstones, with the sandstones frequently displaying trough and planar cross-bedding patterns. This Fm. includes dominant white or light-yellow sandy components. In addition, the Fm. encompasses massive and laminated sandy mudstones, with limestone clasts being a notable constituent within the sandy strata. While the primary lithology of the Stupava Fm. is consistent, it occasionally presents more diverse rock types, including massive or graded conglomerates of varying sizes and compositions, often dominated by bioclasts. Moreover, massive or laminated mudstones are observed, but less frequently than the predominant sand and sandstone layers.

Biostratigraphy/fossils: The Stupava Fm. is rich in calcareous nannofossils (*C. miopelagicus*, *C. macintyrei*, *H.*

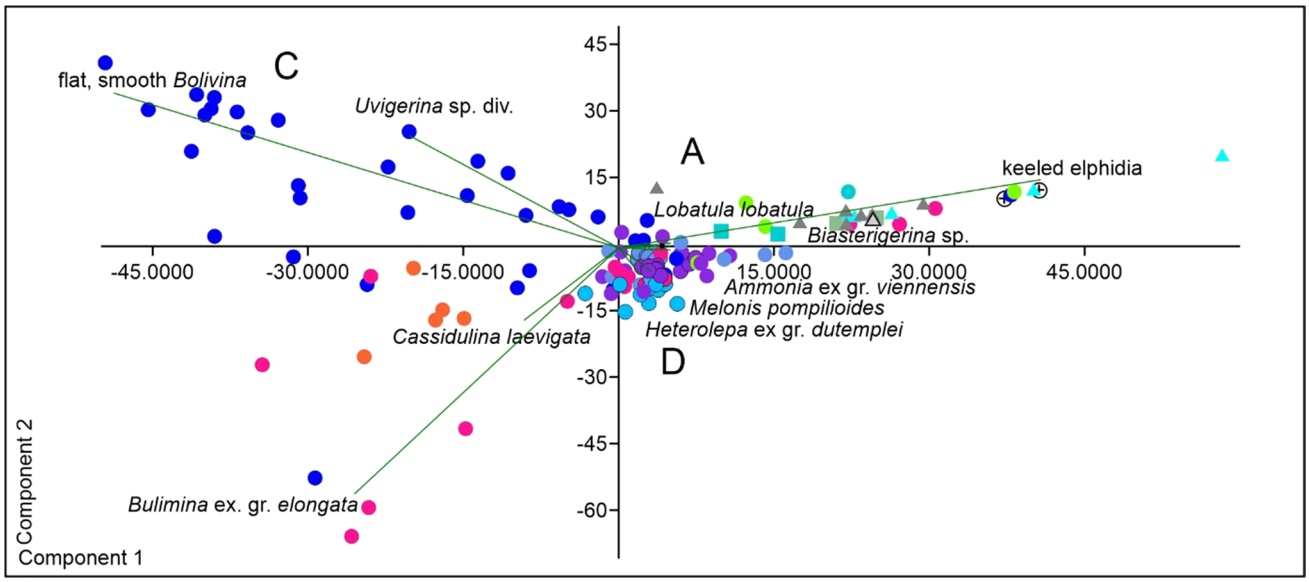

Fig. 16 PCA biplot analysis of the foraminifera associations entire dataset (new and published data) with dominant taxa expressed by green lines. For explanatory notes, see Fig. 8

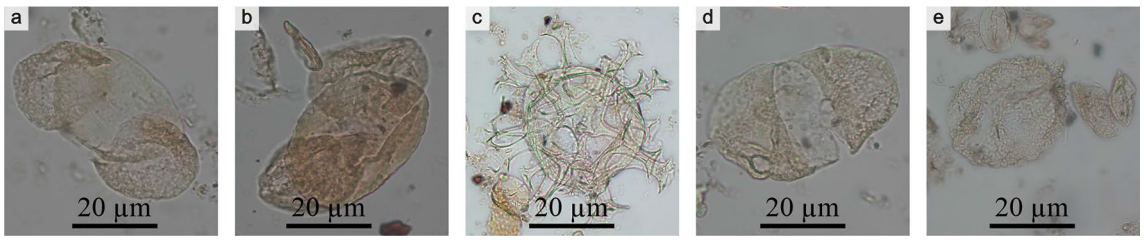

Fig. 17 Palynospectra of ZT6 sample. **a**, **b** *Pinus* sp.; **c** *Achomosphaera* sp.; **d** *Cathaya* sp.; **e** *Tsuga* sp.

walbersdorfensis, *H. wallichii*, *P. japonica*, *S. abies*); benthic foraminifers (*B. melo*, *Miniacina miniacea*, *A. mammilla*, *E. aculeatum*, *B. maxima*, *Bu. intonsa*, *G. bulloides*, *T. quinqueloba*); gastropods (*Turritella tricarinata*); bivalves (*Cubitostrea digitalina*, *Paroxystele orientalis*, *F. leythajanus*, *Oppenheimopecten aduncus*; polyplacophorans; corals; bryozoans; serpulids; echinoderms; ichnofossils; coralline algae (*Lithothamnion*, *Lithophyllum*, *Titanoderma*) (this study, see Supplements 1, 2, 5 in detail).

Depositional environment: The typical depositional depth ranges from ~ 20–50 m (Hrabovský and Fordinál 2013; Pivko et al. 2017; this study). The depositional environment corresponds to a shallow marine setting on the inner shelf, predominantly influenced by tidal and wave actions along the coast. From a sedimentary perspective, it is inferred that the depth did not exceed the normal wave base, with an upper limit ~ 0 m and a lower limit ~ 60 m (bathymetric determination derived from Pellegrini et al. 2020).

Age: Middle Miocene (late Badenian; early Serravallian); younger than 13.8–13.6 Ma up to ~ 12.7 based on NN6 Zone correlation.

Chronometry: Fordinál et al. (2014) reported $^{87}Sr/^{86}Sr$ ages of 13.4–12.8 Ma (Stupava-Vrchná hora) and 13.12–13.02 Ma (Sandberg section).

Overlying unit: The Stupava Fm. crops out on steep hillside inclinations, typically overlaid by the Sandberg Fm. In subsurface instances, the Stupava Fm. is covered by the upper Badenian Sandberg Fm. and by sandy and muddy Holíč and Skalica fms. of Sarmatian age (Vass 2002; Hyžný et al. 2012; Fordinál et al. 2013; this study).

Lateral equivalents: The Rabensburg and Studienka fms., as noted in the Austrian and Slovak territories, signify muddy counterparts within a basinal context (Vass 2002; Fordinál et al. 2013; Harzhauser et al. 2020, 2022). Laterally, the Stupava Fm. sandy facies can transition into shallow water limestones, identified as the Sandberg Fm. (see below), as supported by the present study findings.

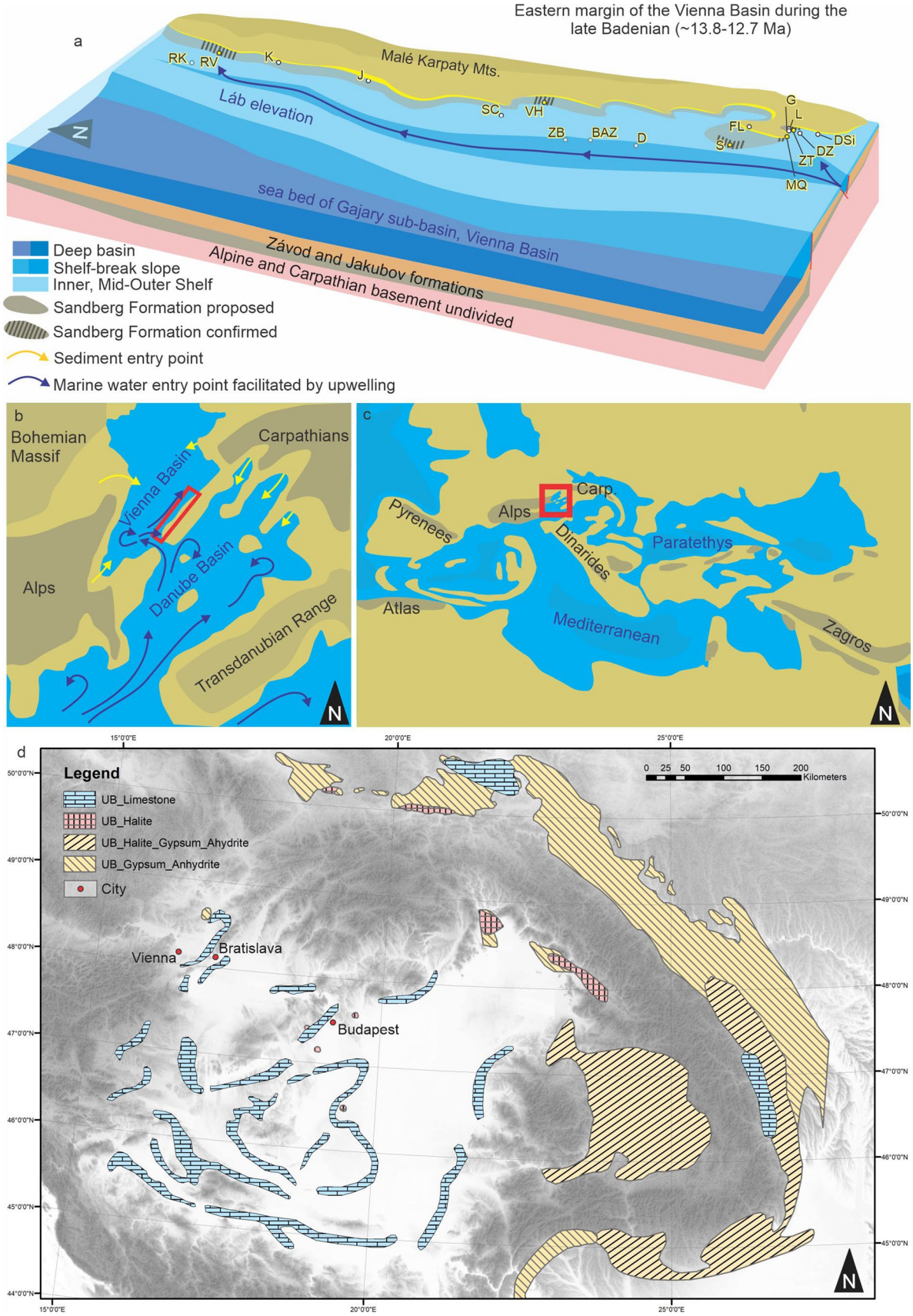
Eastern margin of the Vienna Basin during the late Badenian (~13.8-12.7 Ma)
a
RK
RV
K
J
Malé Karpaty Mts.
Láb elevation
SC
VH
ZB
BAZ
D
FL
S
G
L
DSi
DZ
ZT
MQ
N
sea bed of Gajary sub-basin, Vienna Basin
Závod and Jakubov formations
Alpine and Carpathian basement undivided
Deep basin
Shelf-break slope
Inner, Mid-Outer Shelf
Sandberg Formation proposed
Sandberg Formation confirmed
Sediment entry point
Marine water entry point facilitated by upwelling
b
Bohemian Massif
Carpathians
Vienna Basin
Danube Basin
Alps
Transdanubian Range
N
c
Carp.
Alps
Pyrenees
Dinarides
Paratethys
Atlas
Mediterranean
Zagros
N
d
Legend
UB_Limestone
UB_Halite
UB_Halite_Gypsum_Ahydrite
UB_Gypsum_Anhydrite
City
0 25 50 100 150 200
Kilometers
Vienna
Bratislava
Budapest
15°0'0"E
20°0'0"E
25°0'0"E
50°0'0"N
49°0'0"N
48°0'0"N
47°0'0"N
46°0'0"N
45°0'0"N
44°0'0"N
N

◂**Fig. 18** **a** The late Badenian paleogeographic block diagram of the Vienna Basin's eastern margin suggest the original distribution of the Sandberg Fm. limestones. Explanatory notes: RV—Rohožník Vajarská, RK—Rohožník Konopiská, J—Jabloňové Sandpit, SC—Stupava clay pit, VH—Stupava-Vrchná hora, ZB—Záhorská Bystrica proposed landfill shallow wells, BAZ—Bratislava automobile works, D—Devínska Nová Ves clay pit, S—Devínska Nová Ves Sandberg, FL—Devínska Nová Ves Fuchs quarry, MQ—Devín Medieval quarry, ZT—Devín Zelené Terasy, DZ—Devín Záhrady, DSi—Devín Šibeničný vrch, L—Devín *Lingula* bed, G—Devín *Glossus* bed; **b** a schematic paleogeographic map (after Rybár et al. 2016) of the Vienna and Danube basins demonstrating the inflow of normal marine water (blue arrows) from the "Trans-Tethyan Trench Corridor" (Piller et al. 2007) that supports carbonate growth. It also shows the entry points for clastic sediments (yellow lines) that inhibit carbonate growth. The study area is highlighted in red. **c** Paleogeographic map of the Paratethys Sea (Studencka et al. 1998; Popov et al. 2004; Bartol et al. 2014; Palcu et al. 2017), with the area of interest in red square; **d** distribution map of the upper Badenian limestones and evaporites in/around the Pannonian Basin System. The map indicates areas where carbonate growth was promoted and areas where carbonate growth was hindered due to evaporite precipitation or clastic input (after Steininger et al. 1985; Hámor and Halmai 1988; Peryt and Kasprzyk 1992; Pisera 1996; Sachsenhofer et al. 1998; Popov et al. 2004; Brânzilă and Chira 2005; Harzhauser et al. 2014, 2019, 2020; Hohenegger et al. 2014; Báldi et al. 2017; Kováč et al. 2017a, b, 2018a, b; Pavelić and Kovačić 2018, Mandic et al. 2019a, b; Piller et al. 2022; Babinszki et al. 2023; Piller and Harzhauser 2023)

Geographic distribution: The Stupava Fm. type area is located around the western hill slopes of the Malé Karpaty Mts. (Hrabovský and Fordinál 2013; this study; Figs. 2, 3, 6). The Stupava Fm. also appears along the northern margin of Devín (Hyžný et al. 2012; Pivko et al. 2017; Ruman et al. 2017; this study).

Outcrops: Devín—Zelené Terasy, BAZ, Jabloňové (all in this study), Devín—Medieval quarry (Pivko et al. 2017), Sandberg, DNV—Fuchs quarry, Devín—Šibeničný vrch (all from Hyžný et al. 2012), Devín—Záhrady (Ruman et al. 2017), Stupava-Vrchná hora (Hrabovský and Fordinál 2013).

Definition of the **Sandberg Formation**:

Derivation of name: Named after the hill near Bratislava, "Sandberg Hill."

Synonyms: Limestones of the Sandberg Mb. (Baráth 1993; Vass 2002; Fordinál et al. 2012), St. Margarethen Limestone Harzhauser et al. (2020); Harzhauser (2022a, b, c) and Rákos Limestone of Császár (1997).

Remarks: Certain instances of the Sandberg Fm., particularly at Stupava (Hrabovský and Fordinál 2013), are occasionally misclassified as part of the Leitha Fm. (Harzhauser et al. 2020). This classification is incorrect, given that the Sandberg Fm. dates to the late Badenian (~ 13.8–12.7 Ma) and is correlated with the lower part of NN6 Zone (present study). This implies only a minor overlap (between 13.8 and 13.6 Ma) with the Leitha Fm., which is older and correlated with the NN5 Zone (Wiedl et al. 2013). The minor discrepancy is caused by the NN5/NN6 zonal boundary being set to 13.65 Ma while the Langhian/Serravallian is set to 13.82 Ma Gradstein et al. (2020).

Type section: The summit of the historical Sandberg sandpit near Bratislava (48°12′03″ N, 16°58′29″ E) is in the VB, Záhorie lowland, Slovakia. The Sandberg sandpit is accessible and constitutes a portion of the protected Sandberg—Pajštún Geopark. This section was first described in detail by Švagrovský (1981), then subsequently amended by Baráth (1993), and later biostratigraphically supplemented by Hyžný et al. (2012).

Thickness: As reported by Švagrovský (1981) and Hyžný et al. (2012), the Sandberg Fm. reaches a maximum thickness of 19 m, as evidenced by outcrop data obtained from the western slopes of the Malé Karpaty Mts.

Lithology: The Sandberg Fm. comprises white to cream-colored or light-yellow organodetritic limestones, occasionally featuring coquina-oyster beds. Locally porous, these limestones are filled with cavities resulting from the leaching of gastropod and bivalve shells. Foraminiferal tests and corals may also be present. The Fm. also includes sandy organodetritic limestones with muddy admixtures (Schaleková 1969, 1973, 1978; Benejová 1985; Hladilová 1991; Fordinál et al. 2012; Hrabovský and Fordinál 2013; Zlinská and Madarás 2014).

Biostratigraphy/fossils: The Sandberg Fm. is exceptionally rich in fossils. Calcareous nannofossils (*C. macintyrei*, *H. wallichii*, *S. abies*); benthic foraminifers (*A. mammilla*, *Elphidium crispum*, *B. melo*); echinoids; bryozoans; brachiopods; gastropods (*Turritella tricarinata*, *Paroxystele orientalis*); bivalves; polyplacophorans; coralline algae (*Lithothamnion*, *Lithothamnion minervae*, *L. ramosissimum*, *L. valens*, *L. corallioides*, *Phymatolithon calcareum*, *Spongites albanensis*, *Mesophyllum*, *Lithophyllum*, *Sporolithon*, *Titanoderma pustulatum*, *Hydrolithon*) (this study, see Supplements 1, 2, 5 in detail).

Depositional environment: Shallow marine, inner shelf carbonate ramps, coral carpets, and seagrass meadows. The typical depositional depth ranged from ~ 10 to 30 m (Pivko et al. 2017) to ~ 20–50 m (Hrabovský and Fordinál 2013).

Age: Middle Miocene (late Badenian; early Serravallian); younger than 13.8–13.6 Ma based on NN6 Zone correlation.

Chronometry: Fordinál et al. (2014) reported $^{87}Sr/^{86}Sr$ ages of 13.4–12.8 Ma from the Stupava-Vrchná hora and 12.8–12.6 Ma or 12.7 Ma.

Overlying unit: The Sandberg Fm. typically forms surface outcrops on steep hill slopes, resulting in the erosion of overlying units in most cases. In subsurface occurrences, the Sandberg Fm. is overlain by muddy and sandy Sarmatian deposits from the Holíč and Skalica fms. (Vass 2002; Hyžný et al. 2012).

Lateral equivalents: The Rabensburg and Studienka fms. represent muddy equivalents across Austrian and Slovak territories in basinal and shallow water settings (Vass 2002;

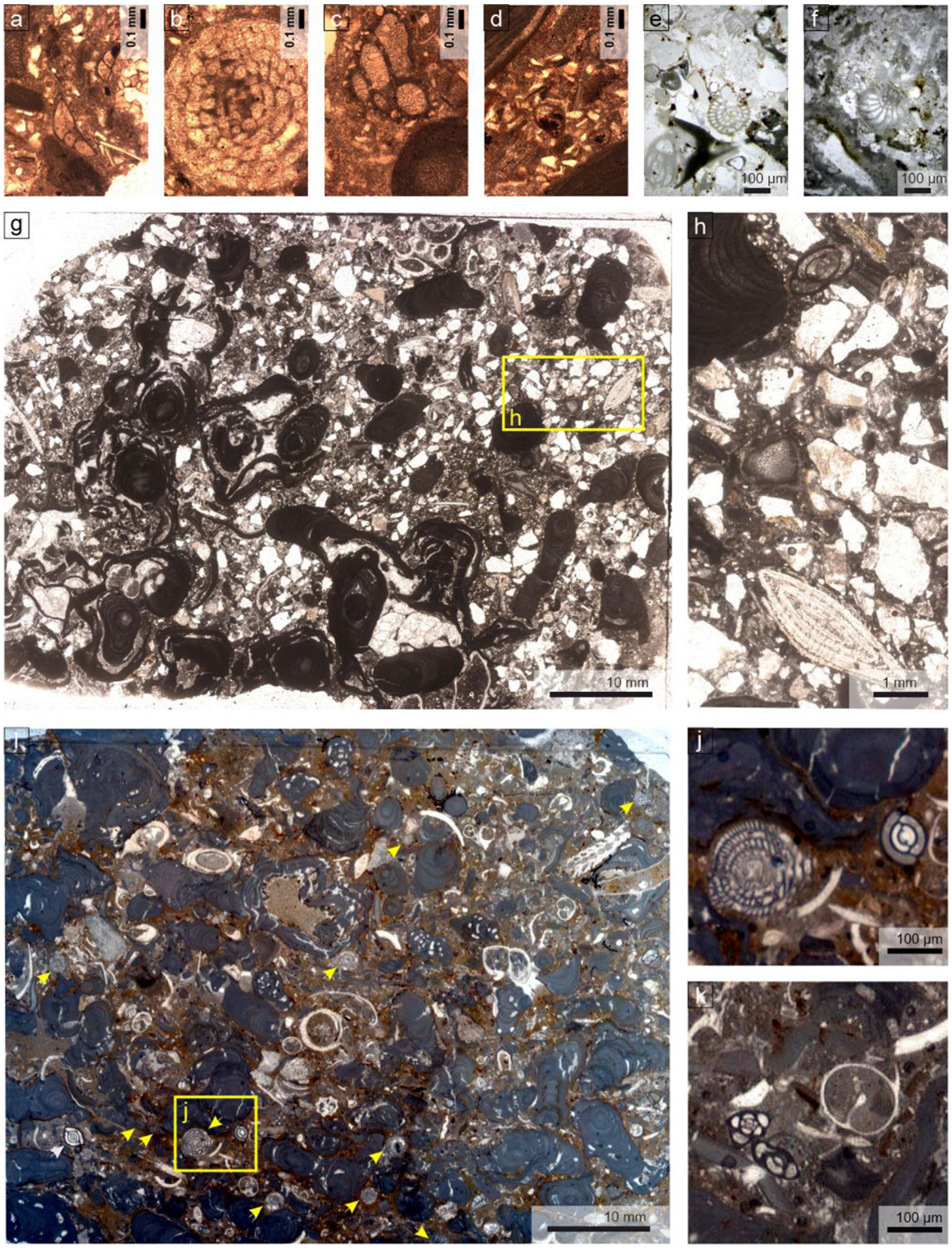

Fig. 19 *Lithothamnion* limestones thin sections. **a** *Lobatula lobatula*, S; **b** *Borelis melo*, S; **c** *Textularia bocki*, S; **d** *Pseudotriloculina* cf. *consobrina*, MQ; **e** *Quinqueloculina* cf. *seminulum*, MQ; **f** *Elphidium crispum*, MQ; **g** *Lithothamnion* limestone thin section, VH; **h** *Amphistegina mamilla*, *Quinqueloculina* sp. indet, VH; **i** *Lithothamnion* limestone thin section, RV; *Borelis melo* (yellow arrows); **j** *Borelis melo*, *Spiroloculina* sp. indet., RV; **k** *Cycloforina badenensis*, gastropod indet., RV

Fordinál et al. 2013; Harzhauser et al. 2020; Harzhauser 2022a, b, c). These facies may be a transition to shallow water and alluvial sands and conglomerates.

Geographic distribution: The Sandberg Fm. type area is located around the western margin of the Malé Karpaty Mts (Fig. 18). These outcrop occurrences are delimited to the west by the approximately NE–SW striking Láb fault line, which extends from Lozorno in the south to Rohožník in the north (Schaleková 1969, 1973, 1978; Benejová 1985; Hladilová 1991; Hrabovský and Fordinál 2013) but they were identified in the deep well Kúty-45 (489–515 m, Kováč et al. 2008a, b) too. The Sandberg Fm. also appears along the northern margin of Devín district (Pivko et al. 2017).

Outcrops: Devín—Zelené Terasy II (this study), DNV—Bratislava automobile works BAZ (this study), DNV—Sandberg sandpit (Hyžný et al. 2012), Devín—Medieval quarry (Pivko et al. 2017), Stupava-Vrchná hora section (this study, new biostratigraphy), and (Hrabovský and Fordinál 2013), Rohožník—Vajarská (Schaleková 1973; Hladilová 1991).

Upper Badenian limestone deposition in the Central Paratethys

During the late Badenian in the CP, the Badenian Salinity Crisis led to the formation of extensive evaporite deposits, primarily gypsum/anhydrite and halite, as highlighted by de Leeuw et al. (2018). These deposits are predominantly found in the Carpathian Foredeep (Pisera 1996; Bąbel and Bogucki 2007) (Fig. 18d), the Transcarpathian (Galamay and Karoli 1997; Vass et al. 2000; Túnyi et al. 2005), and the Transylvanian basins (Krézsek et al. 2010; Beldean et al. 2012). In contrast, the VB and the Pannonian Basin show gypsum/anhydrite in smaller amounts, mostly in cuttings and core samples (Harzhauser et al. 2018, 2020; Kováč et al. 2007; Báldi et al. 2017). These evaporites are intercalated with algal limestones, a pattern seen in the Carpathian Foredeep (Studencki 1979; Peryt and Kasprzyk 1992; Pisera 1996; Szczechura 2000; Brânzilă and Chira 2005; Studencka and Jasionowski 2011). In the Vienna and Pannonian basins, evaporites are less common, blending with muddy and sandy facies, but algal limestones are well developed (Pisera 1996; Magyar et al. 2006; Malvić and Velić 2011; Rundić et al. 2011; Harzhauser et al. 2019, 2020; Piller et al. 2022; Babinszki et al. 2023; Piller and Harzhauser 2023; this study). The Styrian and Danube basins, free from evaporites of this period, feature coralline limestones (Pisera 1996; Schreilechner and Sachsenhofer 2007; Kováč et al. 2018a, b), possibly due to the late Badenian flooding event (Piller et al. 2007). This indicates a deep, broad connection to the global ocean with minimal clastic interference. Thus, basins across the CP, exhibit varying degrees of sea way restriction, ranging from minor (Vienna, Pannonian basins) to major (Carpathian Foredeep, Transcarpathian, and Transylvanian basins), leading to partial or complete circulation cut-offs and subsequent evaporite precipitation. Notably, in the Transylvanian (Krézsek et al. 2010; Beldean et al. 2012) and Transcarpathian basins (Vass 2002), the absence of thick algal limestone deposits suggests presence of significant terrigenous input (e.g., Vass 2000; Klčovo delta) directly above the evaporites, inhibited algal limestone growth. This pattern underscores a dichotomy in the CP basins: some dominated by carbonate growth and others by evaporite deposition.

Conclusion

Our investigation has deployed an integrative approach, employing multiple proxy records, including calcareous nannoplankton, foraminifera, sedimentology, and palynology, to analyze outcrop data of upper Badenian (Serravallian) sediments from the Paratethys Sea shelf. Biostratigraphic dating was conducted based on the presence of *O. rugosus* (ZT9–12, 17, J9), a common occurrence of *H. walbersdorfensis* (ZT5, 8, 9, 11, K1), and the absence of *S. heteromorphus* (observed as reworked in J4, J7). *O. universa* (D, RK) supports these results and aligns with the NN6/CPN9 zones. Our findings accentuate the utility of taphonomic processes and paleoecological proxies for fine-scale characterization and detecting minor fluctuations in paleoenvironmental conditions. One of our key findings is that the distinctive bioherm structures discovered have facilitated the description of limestone formation within the VB (Sandberg Fm.). These limestones are most likely not restricted to the local environment but appear widespread throughout the CP region. The evidence collected supports a substantial connection between the Mediterranean and CP through the Trans-Tethyan Trench Corridor, with the connectivity being strengthened by upwelling conditions observed along the eastern margin of the VB.

Furthermore, our research confirms two primary mechanisms that hindered carbonate growth in the CP area during the late Badenian. The first mechanism was a substantial influx of siliciclastic material from the Alps and Carpathians, resulting from the ongoing rifting of the Vienna and Danube basins. The second mechanism was the initiation of evaporite precipitation in the Transcarpathian and Transylvanian basins, which interrupted normal carbonate growth. In conclusion, this study underlines the crucial interplay between regional geodynamic processes and carbonate sedimentation during the Middle Miocene.

Supplementary Information The online version contains supplementary material available at https://doi.org/10.1007/s10347-023-00679-2.

Acknowledgements Special thanks go to Eva Halásová, Michal Kováč, György Less, Matúš Hyžný, and to our editor Wolfgang Kießling and

reviewers Stjepan Ćorić and those who chose to remain anonymous whose insightful comments improved the manuscript significantly.

Funding Open access funding provided by The Ministry of Education, Science, Research and Sport of the Slovak Republic in cooperation with Centre for Scientific and Technical Information of the Slovak Republic. This study was supported by Agentúra na Podporu Výskumu a Vývoja, APVV-20-0079, APVV-22-0523, APVV-16-0121, Agentúra Ministerstva Školstva, Vedy, Výskumu a Športu SR, VEGA 2/0013/20, VEGA-1/0526/21.

Data availability The authors declare that the data supporting the findings of this study are available within this paper.

References

Andreeva-Grigorovich AS (1998) Ekogrupy nannoplanktonu z verchnebadenskich i nyzhne sarmatskich vidkladiv Predkarpatia. Paleontologičnyj Zbirnyk 32:63–69

Aubry MP (1992) Late Paleogene calcareous nannoplankton evolution: a tale of climatic deterioration. In: Prothero DR, Berggren WA (eds) Eocene-Oligocene climatic and biotic evolution. Princeton University Press, pp 272–309

Auer G, Piller WE, Harzhauser M (2014) High-resolution calcareous nannoplankton palaeoecology as a proxy for small-scale environmental changes in the Early Miocene. Mar Micropaleontol 111:53–65. https://doi.org/10.1016/j.marmicro.2014.06.005

Bąbel M, Bogucki A (2007) The Badenian evaporite basin of the northern Carpathian Foredeep as a model of a meromictic selenite basin. In: Schreiber BC, Lugli S, Bąbel M (eds) Evaporites through space and time, vol 285. Geological Society London, Special Publications, pp 219–246. https://doi.org/10.1144/SP285.13

Babinszki E, Piros O, Csillag G, Fodor L, Gyalog L, Kercsmár Z, Less G, Lukács R, Sebe K, Selmeczi I, Szepesi J, Sztanó O (2023) Magyarország litosztratigráfiai egységeinek leírása II. Kainozoos képződmények, Budapest

Báldi K, Hohenegger J (2008) Paleoecology of benthic foraminifera of the Baden-Sooss section (Badenian, Middle Miocene, Vienna Basin, Austria). Geol Carpath 59(5):411–424

Báldi K, Velledits F, Ćorić S, Lemberkovics V, Lőrincz K, Shevelev M (2017) Discovery of the Badenian evaporites inside the Carpathian Arc: implications for global climate change and Paratethys salinity. Geol Carpath 68(3):193–206. https://doi.org/10.1515/geoca-2017-0015

Báldi-Béke M (1984) A dunántúli paleogén képzodmények nannoplaktonja. Geol Hung Ser Paleontol 43:1–307

Baráth I, Nagy A, Kováč M (1994) Sandberg member-late Badenian marginal sediments on the Eastern Margin of the Vienna Basin. Geologické Práce, Správy 99:59–66 (**in Slovak with English summary**)

Baráth I (1993) Vrchnobádenský rífový komplex na východnom okraji Viedenskej panvy. ln: Hamršmíd B (ed) Nové výsledky v terciéru Západných Karpát (Sborník referátů z 10. konference o mladším terciéru, Brno, 27. - 28. 4. 1992). Knihovnička ZPN 15:177–197

Baráth I (2009) Sedimentologický opis vybratých lokalít neogénnych a kvartérnych sedimentov v južnej časti Záhorskej nížiny. In: Fordinál K, Maglay J, Nagy A, Polák M, Filo I, Olšavský M, Plašienka D, Kohút M, Bezák V, Németh Z, Ábelová M, Šimon L, Kollárová V, Kováčiková M (eds) Vysvetlivky ku geologickým mapám v M 1 : 25 000 listov: 44–232 Devín, 44–241 Bratislava-Karlova Ves (časť), 44–214 Bratislava-Devínska Nová Ves, 44–223 Bratislava-Záhorská Bystrica (časť), 44–212 Zohor, 44–221 Stupava (časť), 34–434 Záhorská Ves, 34–443 Jabloňové (časť), 34–444 Modra-Harmónia (časť). Manuskript. Štátny geologický ústav Dionýza Štúra, Bratislava

Bartol M, Pavšič J, Dobnikar M, Bernasconi SM (2008) Unusual Braarudosphaera bigelowii and Micrantholithus vesper enrichment in the Early Miocene sediments from the Slovenian Corridor, a seaway linking the Central Paratethys and the Mediterranean. Palaeogeogr Palaeoclimatol Palaeoecol 267(1–2):77–88. https://doi.org/10.1016/j.palaeo.2008.06.005

Bartol M, Mikuž V, Horvat A (2014) Palaeontological evidence of communication between the Central Paratethys and the Mediterranean in the late Badenian/early Serravalian. Palaeogeogr Palaeoclimatol Palaeoecol 394:144–157. https://doi.org/10.1016/j.palaeo.2013.12.009

Beldean C, Filipescu S, Bãlc R (2012) Paleoenvironmental and biostratigraphic data for the Early Miocene of the north-western Transylvanian Basin based on planktonic foraminifera. Carpath J Earth Environ Sci 7(1):171–184

Benejová I (1985) Faciálna analýza bádenských litotamniových vápencov na lokalite Rohožník. Diplomová práca, Manuskript. Štátny geologický ústav Dionýza Štúra, Bratislava

Bitner MA, Zágoršek K, Halásová E, Hudáčková N, Jamrich M (2014) Brachiopods and bryozoans from the Sandberg section (Vienna Basin, Central Paratethys) and their significance for environmental interpretation of the Early Sarmatian (= Middle Miocene) Sea. Neues Jahrbuch Für Geologie Und Paläontologie, Stuttgart 273(2):207–219. https://doi.org/10.1127/0077-7749/2014/0424

Boggs S Jr (2006) Principles of Sedimentology and Stratigraphy. 4th ed. Pearson Prentice Hall, Upper Saddle River

Bown PR (1998) Calcareous Nannofossil Biostratigraphy. British Micropalaeontological Society, Publications Series, Chapman and Hall, London

Brânzilă M, Chira C (2005) Microfossils assemblages from the Badenian/Sarmatian boundary in boreholes from the Moldavian Platform. Acta Palaeontolog Rom 5:17–26

Březina J, Alba DM, Ivanov M, Hanáček M, Luján ÁH (2021) A middle Miocene vertebrate assemblage from the Czech part of the Vienna Basin: Implications for the paleoenvironments of the Central Paratethys. Palaeogeogr Palaeoclimatol Palaeoecol 575:110473. https://doi.org/10.1016/j.palaeo.2021.110473

Cachão M, Moita MT (2000) Coccolithus pelagicus, a productivity proxy related to moderate fronts off Western Iberia. Mar Micropaleontol 39:131–155. https://doi.org/10.1016/S0377-8398(00)00018-9

Cicha I, Baldi T, Brzobohatý R, Bůžek Č, Čtyřoká J, Fejfar O, Gabrielová N, Holý F, Jiříček R, Knoblch E, Kvaček Z, Lehotayová R, Molčíková V, Němejc F, Planderová E, Řeháková Z, Seneš J, Sitár V, Slávik J, Steininger F, Švagrovský J, Vaňová M, Vass P, Zapletalová I (eds) (1975) Biozonal division of the Upper Tertiary Basins of the Eastern Alps and Western Carpathians. Geological Survey, Prague, p 147

Cicha I, Rögl F, Rupp C, Čtyroká J (1998) Oligocene-Miocene foraminifera of the central Paratethys. Abhandlungen Der Senckenbergischen Naturforschenden Gesellschaft 549:1–325

Čierna E (1973) Mikropalaontologische und biostratigraphische Untersuchung einiger Bohrproben aus der weiteren Umgebung von Rohožník. Acta Geologica Et Geographica Universitatis Comenianae Bratislava 26:113–187

Cimerman F, Drobne K, Ogorelec B (1988) L`association de foraminifères benthiques des vases de la Baie de Veliko Jezero sur Γ`lle de Mljet et de la Falaise Lenga, ouverte vers la mer (Adriatique Moyenne). In Benthos 86, 3ème Symposium International sur les Foraminifères Benthiques. Reveu de Palèobiologie, Museum d` Histoire Naturelle. Genève 2:741–753

Coe AL (2003) The sedimentary record of sea-level change. Cambridge University Press

Ćorić S, Hohenegger J (2008) Quantitative analyses of calcareous nannoplankton assemblages from the Baden-Sooss section (Middle Miocene of Vienna Basin, Austria). Geol Carpath 59(5):447–460

Császár G (1997) Basic lithostratigraphic units of Hungary, charts and short descriptions. Geological Institute of Hungary, Budapest

Csibri T, Ruman A, Hlavatá Hudáčková N, Jamrich M, Sliva Ľ, Šarinová K, Kováč M (2022) Deltaic systems of the northern Vienna Basin: The lower-middle Miocene conglomerate bodies. Geol Carpath 73(3):245–269. https://doi.org/10.31577/GeolCarp.73.3.5

de Leeuw A, Tulbure M, Kuiper KF, Melinte-Dobrinescu MC, Stoica M, Krijgsman W (2018) New $^{40}Ar/^{39}Ar$, magnetostratigraphic and biostratigraphic constraints on the termination of the Badenian Salinity Crisis: Indications for tectonic improvement of basin interconnectivity in Southern Europe. Global Planet Change 169:1–15. https://doi.org/10.1016/j.gloplacha.2018.07.001

Doláková N, Kováčová M, Utescher T (2021) Vegetation and Climate changes during the Miocene Climatic Optimum (MCO) and Miocene Climatic Transition (MCT) in the northwestern part of Central Paratethys. Geol J 56(2):729–743. https://doi.org/10.1002/gj.4056

Fontanier C, Jorissen FJ, Licari L, Alexandre A, Anschutz P, Carbonel P (2002) Live benthic foraminiferal faunas from the Bay of Biscay: faunal density, composition, and microhabitats. Deep-Sea Res Part I 49(4):751–785. https://doi.org/10.1016/S0967-0637(01)00078-4

Fordinál K, Maglay J, Elečko M, Nagy A, Moravcová M, Vlačiky M, Kohút M, Németh Z, Bezák V, Polák M, Plašienka D, Olšavský M, Buček S, Havrila M, Hók J, Pešková I, Kucharič Ľ, Kubeš P, Malík P, Baláž P, Liščák P, Madarás J, Šefčík P, Baráth I, Boorová D, Uher P, Zlinská A, Žecová K (2012) Explanatory notes to the Geological map of Záhorská nížina at a scale 1:50,000. Štátny Geologický Ústav Dionýza Štúra, Bratislava 1–232

Fordinál K, Maglay J, Nagy A, Elečko M, Vlačiky M, Moravcová M, Zlinská A, Baráth I, Boorová D, Žecová K, Šimon L (2013) Nové poznatky o stratigrafii a litologickom zložení neogénnych a kvartérnych sedimentov regiónu Záhorská nížina. Geologické Práce Správy 121:47–87

Fordinál K, Kráľ J, Harčová E, Čech P, Zieliński G, Nagy A (2014) $^{87}Sr/^{86}Sr$, $\delta^{13}C$ and $\delta^{18}O$ in mollusc fossil shells from marine, brackish and freshwater environments from the Western Carpathians Tertiary sequences. Mineral Slov 46(1–2):23–44 (**(in Slovak with English summary)**)

Fuksi T (2012) Trofická štruktúra spoločenstva mäkkýšov vrchného bádenu z vrtov v okolí Rohožníka (Viedenská panva). Študentská vedecká konferencia 1104–1109

Fuksi T (2015) Multivariate paleoecological analyses of Badenian and Sarmatian molluscan assemblages from the NW Vienna Basin (Rohožník-Konopiská, Slovakia). Geol Geophys Environ 41(1):80–81. https://doi.org/10.7494/geol.2015.41.1.80

Fuksi T, Tomašových A, Rušin Ľ (2016) Regional-scale variation in size and abundance of the bivalve Varicorbula (Middle Miocene, Central Paratethys). EGU General Assembly 2016, Geophysical Research Abstracts, Vol. 18, EGU2016–6721

Galamay AR, Karoli S (1997) Geochemical peculiarities of Badenian salts from East-Slovakian basin. Slovak Geological Magazine 3(3):187–192

Hallock P (1985) Why are larger foraminifera large? Paleobiology 11(2):195–208. https://doi.org/10.1017/S0094837300011507

Hammer Ø, Harper DAT, Ryan PD (2001) PAST. Paleontological Statistics Software Package for Education and Data Analysis. Palaeontologia Electronica 4(1):9. http://palaeo-electronica.org/2001_1/past/issue1_01.htm

Hámor G, Halmai J (eds) (1988) Neogene Palaeogeographic Atlas of Central and Eastern Europe, 7 maps. Hungarian Geological Institute, Budapest

Haq BU (1980) Biogeographic History of Miocene Calcareous Nannoplankton and Paleoceanography of the Atlantic Ocean. Micropaleontology 26(4):414–443

Haq BU, Hardenbol J, Vail PR (1988) Mesozoic and Cenozoic chronostratigraphy and cycles of sea level changes. In: Wilgus CK (ed) Sea-level changes—an integrated approach, vol 42. Society of Economic Paleontologists and Mineralogists, SEPM Special Publication, Tulsa, pp 71–108. https://doi.org/10.2110/pec.88.01.0071

Hardenbol J, Thierry J, Farley MB, Jacquin T, de Graciansky P-C, Vail PR (1998) Mesozoic and Cenozoic sequence chronostratigraphic framework of European basins. In: de Graciansky P-C, Hardenbol J, Jacquin T, Vail PR (eds) Mesozoic and Cenozoic sequence stratigraphy of European Basins, vol 60. Society for Sedimentary Geology. Special Publication, Tulsa, pp 3–13. https://doi.org/10.2110/pec.98.02.0003

Harzhauser M (2022a) Vienna Basin, Korneuburg Basin In: Piller WE (ed) Friebe JG, Gross M, Harzhauser M, Van Husen D, Koukal V, Krenmayr HG, Krois P, Nebelsick JH, Ortner H, Piller WE, Reitner JM, Roetzel R, Rögl F, Rupp C, Stingl V, Wagner L, Wagreich M 2022. The lithostratigraphic units of Austria: Cenozoic Era(them). Abhandlungen der Geologische Bundesanstalt, 76, 163–181

Harzhauser M (2022b) Eisenstadt-Sopron Basin. In: Piller WE (ed) Friebe JG, Gross M, Harzhauser M, Van Husen D, Koukal V, Krenmayr HG, Krois P, Nebelsick JH, Ortner H, Piller WE, Reitner JM, Roetzel R, Rögl F, Rupp C, Stingl V, Wagner L, Wagreich M 2022. The lithostratigraphic units of Austria: Cenozoic Era(them). Abhandlungen der Geologische Bundesanstalt, 76, 181–183

Harzhauser M (2022c) Oberpullendorf Basin (northern margin). In: Piller WE (ed) Friebe JG, Gross M, Harzhauser M, Van Husen D, Koukal V, Krenmayr HG, Krois P, Nebelsick JH, Ortner H, Piller WE, Reitner JM, Roetzel R, Rögl F, Rupp C, Stingl V, Wagner L, Wagreich M 2022. The lithostratigraphic units of Austria: Cenozoic Era(them). Abhandlungen der Geologische Bundesanstalt, 76, 183–186

Harzhauser M, Piller WE (2004) Integrated stratigraphy of the Sarmatian (Upper Middle Miocene) in the western Central Paratethys. Stratigraphy 1(1):65–86

Harzhauser M, Peckmann J, Birgel D, Draganits E, Mandic O, Theobalt D, Huemer J (2014) Stromatolites in the Paratethys Sea during the Middle Miocene climate transition as witness of the Badenian salinity crisis. Facies 60:429–444. https://doi.org/10.1007/s10347-013-0391-z

Harzhauser M, Grunert P, Mandic O, Lukeneder P, García Gallardo Á, Neubauer TA, Carnevale G, Landau BM, Sauer R, Strauss P (2018) Middle and late Badenian palaeoenvironments in the

northern Vienna Basin and their potential link to the Badenian Salinity Crisis. Geol Carpath 69(2):129–168. https://doi.org/10.1515/geoca-2018-0009

Harzhauser M, Theobalt D, Strauss P, Mandic O, Piller WE (2019) Seismic-based lower and middle Miocene stratigraphy in the northwestern Vienna Basin (Austria). Newslett Stratigr 52(2):221–247. https://doi.org/10.1127/nos/2018/0490

Harzhauser M, Kranner M, Mandic O, Strauss P, Siedl W, Piller WE (2020) Miocene lithostratigraphy of the northern and central Vienna Basin (Austria). Austr J Earth Sci 113:169–199. https://doi.org/10.17738/ajes.2020.0011

Haynes JR (1981) Foraminifera. MacMillan, London

Hayward BW, Le Coze F, Vachard D, Gross O (2023) World Foraminifera Database. Accessed at https://www.marinespecies.org/foraminifera on 2023–04–27. https://doi:https://doi.org/10.14284/305

Hilbrecht H (1996) Extant planktic foraminifera and the physical environment in the Atlantic and Indian Oceans. Mitteilungen Aus Dem Geologischen Institut Der Eidgenossenschaftlichen Technischen Hochschule Und Der Universität Zürich, Neue Folge 300:93

Hilgen FJ, Lourens LJ, Van Dam JA (2012) The Neogene period. In: Gradstein FM, Ogg JG, Schmitz MD, Ogg G (eds) A geologic time scale 2012. Elsevier, Amsterdam, pp 923–978

Hladilová Š (1991) Results of preliminary studies of the molluscan fauna from the Rohožník locality. Ser Geol Leiden 21:91–97

Hladilová Š, Hladíková J, Kováč M (1998) Stable Isotope record in Miocene Fossils and Sediments from Rohožník (Vienna Basin, Slovakia). Slov Geol Mag 4(2):87–94

Hoffman A (1977) Synecology of macrobenthic assemblages of the Korytnica Clays (Middle Miocene; Holy Cross Mountains, Poland). Acta Geol Pol 27(2):227–280

Hoffman A (1979) A consideration upon macrobenthic assemblages of the Korytnica Clays (Middle Miocene; Holy Cross Mountains, Central Poland). Acta Geol Pol 29(3):345–352

Hohenegger J, Ćorić S, Wagreich M (2014) Timing of the Middle Miocene Badenian Stage of the Central Paratethys. Geol Carpath 65(1):55–66. https://doi.org/10.2478/geoca-2014-0004

Holcová K (1999) Postmortem transport and resedimentation of foraminiferal tests: relations to cyclical changes of foraminiferal assemblages. Palaeogeogr Palaeoclimatol Palaeoecol 145:157–182. https://doi.org/10.1016/S0031-0182(98)00100-X

Holec P, Emry RJ (2003) Another Molar of the Miocene Hominid Griphopithecus suessi from the Type locality at Sandberg, Slovakia. In: Flynn LJ (ed) Vertebrate Fossils and their Context, Contributions in Honour of Richard H. Tedford. Bulletin of the American Museum of Natural History 279:625–631.

Hrabovský J (2013) Negenikulátne riasy (Corallinales, Sporolithales, Rhodophyta) z litotamniových vápencov lokality Vrchná hora pri Stupave (Viedenská panva, Slovensko). Mineralia Slovaca 45:23–34

Hrabovský J, Fordinál K (2013) Paleoekologické zhodnotenie riasových vápencov z lokality Stupava-Vrchná hora (Viedenská panva, Slovensko). Mineral Slov 45:11–22

Hudáčková N, Hudáček J (2001) Databáza fosílií—technické spracovanie. Mineral Slov Geovestník 33(2):24

Hudáčková N, Kováč M (1993) Zmeny sedimentačného prostredia východnej časti Viedenskej panvy vo vrchnom bádene a sarmate, [The Upper Badenian-Sarmatian events in the area of the Vienna Basin eastern margin]. Mineral Slov 25:202–210

Hudáčková N, Halásová E, Fordinál K, Sabol M, Joniak P, Kráľ J (2003) Biostratigraphy and radiometric dating in the Vienna Basin Neogene (Slovak part). Slovak Geol Mag 9(4):233–235

Hudáčková N, Halásová E, Kováčová M, Rybár S, Kováč M (2013) High resolution study of the holotype locality of the CPN8 Zone (*Globigerina druryi—Globigerina decoraperta*). 14th Czech-Slovak-Polish Paleontological Conference and 9th Micropalaeontological Workshop MIKRO 2013, Grzybowski Foundation Kraków 23

Hudáčková N, Babejová-Kmecová J, Heteš A, Nesterenko O, Hupka R, Zervanová J (2021) Stratigrafické a paleoekologické vyhodnotenie asociácií dierkavcov z vrtu HC-4 (Holíč, Viedenská panva). Geologické Práce Správy 137:3–18

Hyžný M, Hudáčková N, Biskupič R, Rybár S, Fuksi T, Halásová E, Zágoršek K, Jamrich M, Ledvák P (2012) Devínska Kobyla—a window into the Middle Miocene shallow-water marine environments of the Central Paratethys (Vienna Basin, Slovakia). Acta Geol Slov 4(2):95–111

Ivančič K, Trajanova M, Ćorić S, Rožič B, Šmuc A (2018) Miocene paleogeography and biostratigraphy of the Slovenj Gradec Basin: a marine corridor between the Mediterranean and Central Paratethys. Geol Carpath 69(6):528–544. https://doi.org/10.1515/geoca-2018-0031

Jamrich M, Halásová E (2010) The evolution of the Late Badenian calcareous nannofossil assemblages as a reflexion of the palaeoenvironmental changes of the Vienna Basin (Devínska Nová Ves—clay pit). Acta Geol Slov 2(2):123–140

Kaiho K (1994) Benthic foraminiferal dissolved-oxygen index and dissolved-oxygen levels in the modern ocean. Geology 22:719–722

Kováč M (2000) Geodynamický, paleogeografický a štruktúrny vývoj karpatsko-panónskeho regiónu v miocéne: nový pohľad na neogénne panvy Slovenska. Veda, Bratislava

Kováč M, Baráth I, Harzhauser M, Hlavatý I, Hudáčková N (2004) Miocene depositional systems and sequence stratigraphy of the Vienna Basin. Cour Forschungsinst Senck 246:187–212

Kováč M, Andreyeva-Grigorovich A, Bajraktarević Z, Brzobohatý R, Filipescu S, Fodor L, Harzhauser M, Nagymarosy A, Oszczypko N, Pavelić D, Rögl F, Saftić B, Sliva Ľ, Studencka B (2007) Badenian evolution of the Central Paratethys Sea: paleogeography, climate and eustatic sea-level changes. Geol Carpath 58(6):579–606

Kováč M, Sliva Ľ, Sopková B, Hlavatá J, Škulová A (2008a) Serravallian sequence stratigraphy of the Vienna Basin: high frequency cycles in the Sarmatian sedimentary record. Geol Carpath 59(6):545–561

Kováč M, Hudáčková N, Hlavatá J, Sopková B, Grigorovič AA, Halásová E, Kováčová M, Kováčová P, Sliva Ľ, Baráth I (2008b) Miocénne usadeniny vo vrtoch z regiónu Záhorská nížina: sedimentológia, biostratigrafické zaradenie a prostredie depozície. Geologické Práce Správy ŠGUDŠ 114:7–49

Kováč M, Hudáčková N, Halásová E, Kováčová M, Holcová K, Oszczypko-Clowes M, Báldi K, Less G, Nagymarosy A, Ruman A, Klučiar T, Jamrich M (2017a) The Central Paratethys palaeoceanography: a water circulation model based on microfossil proxies, climate, and changes of depositional environment. Acta GeolSlov 9(2):75–114

Kováč M, Márton E, Oszczypko N, Vojtko R, Hók J, Králiková S, Plašienka D, Klučiar T, Hudáčková N, Oszczypko-Clowes M (2017b) Neogene palaeogeography and basin evolution of the Western Carpathians, Northern Pannonian domain and adjoining areas. Global Planet Change 155:133–154. https://doi.org/10.1016/j.gloplacha.2017.07.004

Kováč M, Halásová E, Hudáčková N, Holcová K, Hyžný M, Jamrich M, Ruman A (2018a) Towards better correlation of the Central Paratethys regional time scale with the standard geological time scale of the Miocene Epoch. Geol Carpath 69(3):283–300. https://doi.org/10.1515/geoca-2018-0017

Kováč M, Rybár S, Halásová E, Hudáčková N, Šarinová K, Šujan M, Baranyi V, Kováčová M, Ruman A, Klučiar T, Zlinská A (2018b) Changes in Cenozoic depositional environment and sediment provenance in the Danube Basin. Basin Res 30(1):97–131. https://doi.org/10.1111/bre.12244

Kováčová P, Hudáčková N (2009) Late Badenian foraminifers from the Vienna Basin (Central Paratethys): Stable isotope study and paleoecological implications. Geol Carpath 60(1):59–70. https://doi.org/10.2478/v10096-009-0006-3

Kranner M, Harzhauser M, Mandic O, Strauss P, Siedl W, Piller WE (2021a) Early and middle Miocene paleobathymetry of the Vienna Basin (Austria). Mar Pet Geol 132:105187. https://doi.org/10.1016/j.marpetgeo.2021.105187

Kranner M, Harzhauser M, Mandic O, Strauss P, Siedl W, Piller WE (2021b) Trends in temperature, salinity and productivity in the Vienna Basin (Austria) during the early and middle Miocene, based on foraminiferal ecology. Palaeogeogr Palaeoclimatol Palaeoecol 581:110640. https://doi.org/10.1016/j.palaeo.2021.110640

Krézsek C, Filipescu S, Silye L, Maţenco L, Doust H (2010) Miocene facies associations and sedimentary evolution of the Southern Transylvanian Basin (Romania): Implications for hydrocarbon exploration. Mar Pet Geol 27(1):191–214. https://doi.org/10.1016/j.marpetgeo.2009.07.009

Krijgsman W, Piller WE (2012) Regional stages. Central and Eastern Paratethys. In: Gradstein FM, Ogg JG, Schmitz MD, Ogg G (eds) A geologic time scale 2012. Elsevier, Amsterdam, pp 935–937

Kysela J (1988) Microfacies, porosity types of the Leitha limestones and Upper Triassic dolomites underlying the Vienna basin. Západné Karpaty, séria geológia 13. Geologický ústav Dionýza Štúra, Bratislava

Lee EJ, Wagreich M (2017) Polyphase tectonic subsidence evolution of the Vienna Basin inferred from quantitative subsidence analysis of the northern and central parts. Int J Earth Sci 106:687–705. https://doi.org/10.1007/s00531-016-1329-9

Lehotayová R (1989) The calcareous nannoplankton of Badenian deposits from the borehole Devínska Nová Ves-1. Západné Karpaty Séria Paleontológia 13:61–68

Less G (2020) Új sr-izotóp koradatok a középső paratethysből és Értelmezésük. Műszaki Földtudományi Közlemények 89(2):252–257

Lukács R, Harangi S, Bachmann O, Guillong M, Danišík M, Buret Y, von Quadt A, Dunkl I, Fodor L, Sliwinski J, Soós I, Szepesi J (2015) Zircon geochronology and geochemistry to constrain the youngest eruption events and magma evolution of the Mid-Miocene ignimbrite flare-up in the Pannonian Basin, eastern central Europe. Contrib Miner Petrol 170(5):52. https://doi.org/10.1007/s00410-015-1206-8

Magyar I, Fogarasi A, Vakarcs G, Bukó L, Tari GC (2006) The largest hydrocarbon field discovered to date in Hungary: Algyő. In: Golonka J and Picha FJ (eds) The Carpathians and their foreland: geology and hydrocarbon resources. American Association of Petroleum Geologists AAPG Memoir 84: 619–632. https://doi.org/10.1306/985734M843142

Malvić T, Velić J (2011) Neogene Tectonics in Croatian Part of the Pannonian Basin and Reflectance in Hydrocarbon Accumulations. In: Schattner U (ed) New frontiers in tectonic research—at the midst of plate Convergence. IntechOpen. https://doi.org/10.5772/21270

Mandic O, Harzhauser M (2003) Molluscs from the Badenian (Middle Miocene) of the Gaindorf Formation (Alpine Molasse Basin, NE Austria)—Taxonomy, Paleoecology and Biostratigraphy. Annalen Des Naturhistorischen Museums in Wien 104A:85–127

Mandic O, Sant K, Kallanxhi M-E, Ćorić S, Theobalt D, Grunert P, De Leeuw A, Krijgsman W (2019a) Integrated bio-magnetostratigraphy of the Badenian reference section Ugljevik in southern Pannonian Basin - implications for the Paratethys history (middle Miocene, Central Europe). Global Planet Change 172:374–395. https://doi.org/10.1016/j.gloplacha.2018.10.010

Mandic O, Rundic L, Ćorić S, Pezelj D, Theobalt D, Sant K, Krijgsman W (2019b) Age and mode of the middle Miocene marine flooding of the Pannonian Basin—constraints from central Serbia. Palaios 34(2):71–95. https://doi.org/10.2110/palo.2018.052

Martini E (1971) Standard Tertiary and Quaternary Calcareous Nannoplankton Zonation. In: Farinacci A (ed) Proceedings of the II Planktonic Conference, Roma, 1970. Edizioni Tecnoscienza 739–785

Mišík M (1974) Geologické exkurzie po Slovensku. Slovenské pedagogické nakladateľstvo. (**in Slovak**)

Mišík M, Reháková D (2009) Vápence Slovenska, I. časť. Biohermné, krinoidové, sladkovodné, ooidové a onkoidové vápence. Veda, Bratislava

Morse JW, Arvidson RS, Lüttge A (2007) Calcium carbonate formation and dissolution. Chem Rev 107(2):342–381. https://doi.org/10.1021/cr050358j

Murray JW (2006) Ecology and Applications of Benthic Foraminifera. Cambridge University Press, New York

Nagy A, Baráth I, Ondrejičková A (1993) Karloveské vrstvy - marginálne sedimenty sarmatu východného okraja Viedenskej panvy. Geologické práce, Správy 97:69–72 **(in Slovak with English summary)**

Nehyba S, Roetzel R (2004) The Hollabrunn—Mistelbach Formation (Upper Miocene, Pannonian) in the Alpine- Carpathian Foredeep and the Vienna Basin in Lower Austria—an example of a Coarse-grained Fluvial System. Jahrb Geol Bundesanst 144:191–221

Nichols G (2009) Sedimentology and stratigraphy, 2nd edn. Wiley-Blackwell, Chichester

Nováková P, Rybár S, Šarinová K, Nagy A, Hudáčková N, Jamrich M, Teodoridis V, Kováčová M, Šujan M, Vlček T, Kováč M (2020) The late Badenian-Sarmatian (Serravallian) environmental transition calibrated by sequence stratigraphy (Eastern Danube Basin, Central Paratethys). Geol Carpath 71(4):291–313. https://doi.org/10.31577/GeolCarp.71.4.1

Palcu DV, Golovina LA, Vernyhorova YV, Popov SV, Krijgsman W (2017) Middle Miocene paleoenvironmental crises in Central Eurasia caused by changes in marine gateway configuration. Global Planet Change 158:57–71. https://doi.org/10.1016/j.gloplacha.2017.09.013

Paulissen WE, Luthi SM (2010) Thematic Set: Integrating magnetostratigraphy, biostratigraphy, cyclostratigraphy and seismic data to obtain a high resolution stratigraphic record: a case study from the Vienna Basin. First Break 28(1):1–18. https://doi.org/10.3997/1365-2397.2010004

Paulissen WE, Luthi SM, Grunert P, Ćorić S, Harzhauser M (2011) Integrated high-resolution stratigraphy of a Middle to Late Miocene sedimentary sequence in the central part of the Vienna Basin. Geol Carpath 62(2):155–169. https://doi.org/10.2478/v10096-011-0013-z

Pavelić D, Kovačić M (2018) Sedimentology and stratigraphy of the Neogene rift-type North Croatian Basin (Pannonian Basin System, Croatia): a review. Mar Pet Geol 91:455–469. https://doi.org/10.1016/j.marpetgeo.2018.01.026

Pellegrini C, Patruno S, Helland-Hansen W, Steel RJ, Trincardi F (2020) Clinoforms and clinothems: fundamental elements of basin infill. Basin Res 32:187–205. https://doi.org/10.1111/bre.12446

Perch-Nielsen K (1985) Cenozoic calcareous nannofossils. In: Bolli HM, Saunders JB, Perch-Nielsen K (eds) Plankton stratigraphy. Cambridge University Press, pp 427–554

Peryt TM, Kasprzyk A (1992) Carbonate-evaporite sedimentary transitions in the Badenian (middle Miocene) basin of southern Poland. Sed Geol 76:257–271. https://doi.org/10.1016/0037-0738(92)90087-8

Piller WE, Harzhauser M (2023) Bryoherms from the lower Sarmatian (upper Serravallian, Middle Miocene) of the Central Paratethys. Facies 69:5. https://doi.org/10.1007/s10347-023-00661-y

Piller WE, Harzhauser M, Mandic O (2007) Miocene Central Paratethys stratigraphy—current status and future directions. Stratigraphy 4(2/3):151–168

Piller WE, Auer G, Graber H, Gross M (2022) Marine facies differentiation along complex paleotopography: an example from the Middle Miocene (Serravallian) of Lower Austria. Swiss J Geosci 115:25. https://doi.org/10.1186/s00015-022-00425-w

Pisera A (1996) Miocene reefs of the Paratethys: A review. In: Franseen EK, Esteban M, Ward WC, Rouchy J-M (eds) Models for carbonate stratigraphy from Miocene reef complexes of Mediterranean regions, vol 5. Society for Sedimentary Geology. Concepts in Sedimentology and Paleontology, Tulsa, pp 97–104

Pivko D, Hudáčková N, Hrabovský J, Sládek I, Ruman A (2017) Palaeoecology and sedimentology of the Miocene marine and terrestrial sediments in the "Medieval quarry" on the Devínska Kobyla hill (Vienna Basin). GeolQuarterly 61(3):549–568. https://doi.org/10.7306/gq.1357

Popov SV, Rögl F, Rozanov AY, Steininger FF, Shcherba IG, Kovac M (2004) Lithological-Paleogeographic maps of Paratethys. 10 Maps Late Eocene to Pliocene: Courier Forschungsinstitut Senckenberg 250:1–46

Pratt DM, Campbell DA (1956) Environmental factors affecting growth in Venus mercenaria. Limnol Oceanogr 1:2–17

Rahman A, Roth PH (1990) Late Neogene Paleoceanography and Paleoclimatology of the Gulf of Aden Region based on Calcareous Nannofossils. Paleoceanography 5(1):91–107

Reynolds L, Thunell RC (1985) Seasonal succession of planktonic foraminifera in the subpolar North Pacific. J Foramin Res 15(4):282–301. https://doi.org/10.2113/gsjfr.15.4.282

Rossi VM, Perillo M, Steel RJ, Olariu C (2017) Quantifying mixed-process variability in shallow-marine depositional systems: what are sedimentary structures really telling us? J Sediment Res 87(10):1060–1074. https://doi.org/10.2110/jsr.2017.49

Ruman A, Hlavatá Hudáčková N (2015) Middle Miocene chitons (Polyplacophora) from the Slovak part of the Vienna Basin and the Danube Basin (Central Paratethys). Acta Geol Slov 7(2):155–173

Ruman A, Rybár S, Hudáčková N, Šujan M, Halásová E (2017) Depositional environment changes at the Early—Late Serravallian boundary dated by the Central Paratethys bioevents. Facies 63(9):1–13. https://doi.org/10.1007/s10347-016-0490-8

Rundić L, Knežević S, Vasić N, Cvetkov V, Rakijaš M (2011) New data concerning the Early Middle Miocene on the southern slopes of Fruška Gora (northern Serbia): a case study from the Mutalj Quarry. Annales Géologiques De La Péninsule Balkanique 72:71–85. https://doi.org/10.2298/GABP1172071R

Rybár S, Kováč M, Šarinová K, Halásová E, Hudáčková N, Šujan M, Kováčová M, Ruman A, Klučiar T (2016) Neogene changes in palaeogeography, palaeoenvironment and the provenance of sediment in the Northern Danube Basin. Bull Geosci 91(2):367–398. https://doi.org/10.3140/bull.geosci.1571

Sabol M, Holec P (2002) Temporal and spatial distribution of Miocene mammals in the Western Carpathians (Slovakia). Geol Carpath 53(4):269–279

Sachsenhofer RF, Rantitsch G, Hasenhüttl C, Russegger B, Jelen B (1998) Smectite to illite diagenesis in early Miocene sediments from the hyperthermal western Pannonian Basin. Clay Miner 33(4):523–537. https://doi.org/10.1180/000985598545778

Salas C (1996) Marine bivalves from off the southern Iberian Peninsula collected by the Balgim and Fauna 1 expeditions. Haliotis 25:33–100

Šarinová K, Hudáčková N, Rybár S, Jamrich M, Jourdan F, Frew A, Mayers C, Ruman A, Subová V, Sliva Ľ (2021) $^{40}Ar/^{39}Ar$ dating and palaeoenvironments at the boundary of the early-late Badenian (Langhian-Serravallian) in the northwest margin of the Pannonian basin system. Facies 67:29. https://doi.org/10.1007/s10347-021-00637-w

Schaleková A (1969) Zur näheren kenntniss der Corallinaceen im Leithacalk des Sandberges bei Devínska Nová Ves (Theben—Neudorf) in der Südwestslowakei. Acta Geol Et Geogr Univ Comenianae Bratislava 18:93–102

Schaleková A (1973) Oberbadenische Corallinaceen aus dem Steinbruch Rohožník - Vajar an dem Westhang der Kleinen Karpaten. Acta Geol Et Geograph Univs ComenianaemBratislava 26:211–221

Schaleková A (1978) Riasové (litotamniové) vápence v bádene Viedenskej, podunajskej a juhoslovenskej panvy Západných Karpát. Habilitačná práca. Manuskript. Štátny geologický ústav Dionýza Štúra, Bratislava

Schmid HP, Harzhauser M, Kroh A, Coric S, Rögl F, Schultz O (2001) Hypoxic events on a Middle Miocene carbonate platform of the Central Paratethys (Austria, Badenian, 14 Ma). Annalen Des Naturhistorischen Museums in Wien 102A:1–50

Schreilechner MG, Sachsenhofer RF (2007) High resolution sequence stratigraphy in the Eastern Styrian Basin (Miocene, Austria). Austr J Earth Sci 100:164–184

Sitár V, Kováčová-Slamková M (1999) Palaeobotanical and palynological study of the upper Badenian sediments from the NE part of the Vienna Basin (locality Devínska Nová Ves). Acta Palaeobotanica Supplement 2:373–389

Soliman A, Piller WE, Dybkjær K, Slimani H, Auer G (2023) Middle Miocene (Serravallian; upper Badenian—lower Sarmatian) dinoflagellate cysts from Bad Deutsch—Altenburg, Vienna Basin, Austria. Palynology 47(1):2116498. https://doi.org/10.1080/01916122.2022.2116498

Spezzaferri S, Ćorić S (2001) Ecology of Karpatian (Early Miocene) foraminifers and calcareous nannoplankton from Laa an der Thaya, Lower Austria: a statistical approach. Geol Carpath 52(6):361–374

Špička V (1966) Palaeogeography and tectonogenesis of the Vienna Basin and contribution to its oil-geological problematics. Rozpravy Československé Akademie Věd Řada Matematických-Přírodopisných Věd 76(12):1–118 (**in Czech**)

Stanley SM (1970) Relation of shell form to life habits in the Bivalvia (Mollusca). The Geological Society of America, Memoir 125

Steininger FF, Seneš J, Kleemann K, Rögl F (eds) (1985) Neogene of the Mediterranean Tethys and Paratethys. In: Stratigraphic correlation tables and sediment distribution maps. Volumes 1: XIV+189 p., 10 maps; 2: XXVI+536 p. Institute of Paleontology, University of Vienna, Vienna

Studencka B, Jasionowski M (2011) Bivalves from the Middle Miocene reefs of Poland and Ukraine: a new approach to Badenian/Sarmatian boundary in the Paratethys. Acta Geol Pol 61(1):79–114

Studencka B, Gontsharova IA, Popov SV (1998) The bivalve fauna as a basis for reconstruction of the Middle Miocene history of the Paratethys. Acta Geol Pol 48(3):285–342

Studencki W (1979) Sedimentation of algal limestones from Busko-spa environs (middle miocene, Central Poland). Palaeogeogr Palaeoclimatol Palaeoecol 27:155–165. https://doi.org/10.1016/0031-0182(79)90098-1

Šujan M (2019) Bratislava naprieč miliónmi rokov—súhra sedimentácie a tektoniky. In: Šimkovič V, Vozárová T (eds) Bratislava a more. Geológia Bratislavy ako inšpirácia architektonickej tvorby. Vydavateľstvo Spektrum STU, Bratislava, pp 29–42 (**in Slovak**)

Šujan M, Modlitba I, Kováč M, Dzúrik J, Hudáčková N, Šucha V, Hrabina J (1992) Komplexný geologický prieskum pre Skládku

škváry a popolčeka. Záverečná správa, archive of the Department of Geology and Paleontology, Comenius University in Bratislava

Švagrovský J (1981) Lithofazielle Entwicklung und Molluskenfauna des oberen Badeniens (Miozän M4d) in dem Gebiet Bratislava—Devínska Nová Ves. Západné Karpaty, Séria Paleontológia 7:5–204

Szczechura J (2000) Age and evolution of depositional environments of the supra-evaporitic deposits in the northern, marginal part of the Carpathian Foredeep: micropalaeontologica1 evidence. Geol Q 44(1):81–100

Túnyi I, Vass D, Karoli S, Janočko J, Halásová E, Zlínská A, Beláček B (2005) Magnetostratigraphy of Badenian evaporite deposits (East Slovak Basin). Geol Carpath 56(3):273–284

Vass D (2002) Lithostratigraphic units of West Carpathians: Neogene and Buda Paleogene. GUDŠ, Bratislava (**in Slovak with English summary**)

Vass D, Elečko M, Janočko J, Karoli S, Pereszlenyi M, Slávik J, Kaličiak M (2000) Palaeogeography of the East-Slovakian Basin. Slovak Geol Mag 6(4):377–407

Vlček T, Kováčová M, Šarinová K, Rybár S, Hudáčková N, Ruman A, Jamrich M, Franců J (2022) Multiproxy constraints on Central Paratethys Sea and Lake Pannon paleoclimate and paleoenvironment transitions during the Middle-Late Miocene (Danube Basin, Slovakia). Palaeogeogr Palaeoclimatol Palaeoecol 600:111058. https://doi.org/10.1016/j.palaeo.2022.111058

Wade BS, Bown PR (2006) Calcareous nannofossils in extreme environments: the Messinian Salinity Crisis, Polemi Basin, Cyprus. Palaeogeogr Palaeoclimatol Palaeoecol 233:271–286. https://doi.org/10.1016/J.PALAEO.2005.10.007

Wade BS, Pearson PN, Berggren WA, Pälike H (2011) Review and revision of Cenozoic tropical planktonic foraminiferal biostratigraphy and calibration to the geomagnetic polarity and astronomical time scale. Earth Sci Rev 104:111–142. https://doi.org/10.1016/j.earscirev.2010.09.003

Walanus A, Nalepka D (1999) Polpal Program for counting pollen grains, diagrams plotting and numerical analysis. Acta Palaeobotanica, Supplementum 2:659–661. http://www.adamwalanus.pl/2017/polpal1999/index.html. https://www.adamwalanus.pl/Polpal.html

Wiedl T, Harzhauser M, Kroh A, Ćorić S, Piller WE (2013) Ecospace variability along a carbonate platform at the northern boundary of the Miocene reef belt Upper Langhian, Austria. Palaeogeogr Palaeoclimatol Palaeoecol 370:232–246. https://doi.org/10.1016/j.palaeo.2012.12.015

Wiedl T, Harzhauser M, Kroh A, Ćorić S, Piller WE (2014) From biologically to hydrodynamically controlled carbonate production by tectonically induced paleogeographic rearrangement (Middle Miocene, Pannonian Basin). Facies 60:865–881. https://doi.org/10.1007/s10347-014-0408-2

Young JR (1998) Calcareous nannofossil biostratigraphy. In: Bown PR (ed) British Micropalaeontological Society, Publications Series. Chapman and Hall, London

Young JR, Bown PR, Lees JA (2017) Nannotax3 website. International Nannoplankton Association. http://www.mikrotax.org/Nannotax3. Accessed 21 Apr 2017

Zlinská A, Madarás J (2014) New biostratigraphical data from the Miocene Paleokarst in the Devín Castle cliff (Slovakia, Malé Karpaty Mts.) In: 9th ESSEWECA Conference, Smolenice, pp 71–72